

Toward optimal-scaling DFT: Stochastic Hartree theory in the thermodynamic and complete basis set limits at arbitrary temperature

Yuhang Cai*

Michael Lindsey*[†]

Abstract

We present the first mathematical analysis of stochastic density functional theory (DFT) in the context of the Hartree approximation. We motivate our analysis via the notion of nearly-optimal or $\tilde{O}(n)$ scaling with respect to the number n of computational degrees of freedom, independent of the number of electrons, in both the thermodynamic and complete basis set limits. Indeed, the promise of such scaling is the primary motivation for stochastic DFT relative to conventional orbital-based approaches, as well as deterministic orbital-free alternatives. We highlight three key targets for mathematical attention, which are synthesized in our algorithm and analysis. First, we identify a particular stochastic estimator for the Hartree potential whose sample complexity is essentially independent of the discretization size. Second, we reformulate the self-consistent field iteration as a stochastic mirror descent method where the Fermi-Dirac entropy plays the role of the Bregman potential, and we prove a nearly discretization-independent bound on the number of iterations needed to reach fixed accuracy. Third, motivated by the estimator, we introduce a novel pole expansion scheme for the square-root Fermi-Dirac operator, preserving $\tilde{O}(n)$ cost per mirror descent iteration even in the complete basis set limit. Combining these ingredients, we establish nearly-optimal scaling in both limits of interest under reasonable assumptions on the basis sets chosen for discretization. Extensive numerical experiments on problems with as many as 10^6 degrees of freedom validate our algorithm and support the theory of nearly-optimal scaling.

1 Introduction

Density functional theory (DFT) [18] is the most widely used computational tool in electronic structure theory, with far-reaching applications across quantum chemistry and materials science. The central idea of DFT is to solve the many-electron problem by way of an effective single-electron problem, whose Hamiltonian is determined self-consistently in terms of the electron density.

This work is a mathematical study of a framework for solving DFT known as stochastic DFT [1, 7, 12], within which we consider certain modifications and extensions. First we review the motivation for this approach, through the lens of a suitable notion of *optimal scaling* on which we shall elaborate. This notion will motivate and guide our algorithms and analysis.

*University of California, Berkeley

[†]Lawrence Berkeley National Laboratory

Conventional approaches to density functional theory at zero temperature rely on finding self-consistent solutions to the Kohn-Sham equations

$$H_{\text{eff}}[\rho] \psi_j = \varepsilon_j \psi_j, \quad j = 1, \dots, N,$$

$$\rho(x) = \sum_{j=1}^N |\psi_j(x)|^2.$$

Here the Kohn-Sham orbitals ψ_j , $j = 1, \dots, N$, are the lowest N orthonormal eigenfunctions of the effective single-particle Hamiltonian

$$H_{\text{eff}}[\rho] := -\frac{1}{2}\Delta + v_{\text{ext}} + v_{\text{hxc}}[\rho],$$

which consists of terms corresponding to the kinetic energy, the fixed external potential, and the Hartree-exchange-correlation potential, respectively. The last of these must be determined self-consistently via the electron density ρ . Moreover, note that N indicates the number of electrons, which is fixed *a priori* in such a zero-temperature setting.

The Kohn-Sham equations must be solved within some kind of framework of discretization. In spite of the diversity of approaches (based, for example, on finite differences, finite elements, or specialized and highly successful quantum chemistry basis sets [33]), roughly speaking one must always incur a cost of at least $O(N^2n)$ where n is the number of grid points or basis functions, simply due to the cost of orthogonalizing the Kohn-Sham orbitals.

As such there is an interest in orbital-free methods that avoid any explicit dependence on N by working with the density matrix

$$P(x, y) = \sum_{j=1}^N \psi_j(x) \psi_j(y),$$

from which the electron density can be recovered as the diagonal. These approaches are also more naturally formulated at finite temperature, which enhances their interest from the point of view, e.g., of warm dense matter (WDM) [38]. The zero-temperature limit can be recovered suitably.

The key idea of such methods is that we can recast the Kohn-Sham equations in the form

$$P = f_\beta (H_{\text{eff}}[\rho] - \mu \mathbf{I})$$

$$\rho = \text{diag}[P],$$

where

$$f_\beta(x) = \frac{1}{1 + e^{\beta x}}$$

is the Fermi-Dirac occupation function at inverse temperature $\beta \in (0, \infty)$, applied in the sense of the continuous operator calculus, and $\mu \in \mathbb{R}$ is a chemical potential.

Recently, PEXSI (pole expansion and selected inversion) [23, 22, 21] has gained popularity as one such orbital-free approach, which, unlike stochastic DFT, is completely deterministic. (We will review the longer history of stochastic orbital-free methods shortly.) The main idea of PEXSI is that the Fermi-Dirac function can be approximated accurately as a sum of only a modest number of poles, and in turn the electron density can be recovered as the sum of diagonals of inverses of

sparse matrices. The selected inversion component of PEXSI achieves this latter step with a direct algorithm while avoiding the formation of the entire inverse matrix. However, the cost is controlled by a suitable fill-in pattern and scales as $O(n^2)$ for grid-based discretizations of general 3D systems. Still, the cost scaling in practice is quite compelling in many practical scenarios, especially for quasi-1D and quasi-2D molecules.

The hope of stochastic DFT is to achieve a method with truly $\tilde{O}(n)$ cost, independent of the electron number, where the tilde indicates the omission of logarithmic factors. This defines a target notion of *optimal scaling*, as the scaling of simply storing the electron density on a grid of n points is $O(n)$. With a view toward achieving this scaling, stochastic DFT constructs an estimator for the electron density on a grid using a stochastic trace estimator. It remains to elucidate additional factors encoding dependence on the target error ε and the inverse temperature β , which we will explain below.

The roots of stochastic DFT go back at least to 1990s [9], and more recent efforts [1, 7, 12, 38, 25] have advanced stochastic DFT as a practical algorithm for *ab initio* electronic structure problems. However, to our knowledge, stochastic DFT has not received any attention from the point of view of mathematical analysis.

In our view, there are several key components deserving of mathematical attention.

1. The **stochastic trace estimator** used for estimating the effective potential. Although several different variations have been tried in the literature (contrast, e.g., [7] and [12]), we demonstrate that one choice in particular admits a nearly-dimension-independent sample complexity, both for grid-based and arbitrary Galerkin discretizations. We comment that several more advanced approaches have been introduced and applied to reduce the variance of the stochastic estimator. These include the embedded-fragments theory [12] which involves a decomposition of the computational domain into local fragments, as well as approaches that mix deterministic and stochastic Kohn-Sham orbitals [38, 25]. While these approaches fall outside the scope dictated by our pursuit of optimal scaling, they can offer significant practical speedups and offer interesting avenues for further theoretical investigation.
2. The **optimization** algorithm for solving the self-consistency criterion. Typically, stochastic DFT is solved via an approach resembling the traditional self-consistent field (SCF) iteration, where a stochastic estimator for the effective potential is dropped in as a replacement for the exact effective potential, and special attention is paid to the chemical potential adjustment [7]. We adopt a novel point of view on SCF through the lens of *mirror descent*, which we shall review below. In short, this perspective allows us to prove a nearly-dimension-independent bound on the number of iterations required to achieve fixed accuracy. We remark that this perspective may also shed light on deterministic SCF, where to our knowledge no analogous dimension-independent results on the convergence rate are known.
3. The **matrix function approximation** used within the trace estimator. We shall see that the aforementioned ‘good’ stochastic trace estimator requires a fast algorithm for matrix-vector products by $f_\beta^{1/2}(H_{\text{eff}})$, where $f_\beta^{1/2}$ denotes the square root of the Fermi-Dirac function. Stochastic DFT typically approaches this task via Chebyshev expansion of $f_\beta^{1/2}$ over the spectral range of H_{eff} [7]. However, as the basis set is refined (per unit volume), i.e., in the *complete basis set limit*, the number of terms in the expansion grows with n due to the fact that the Laplacian term in the effective Hamiltonian is unbounded. As such, we introduce an alternative approach based on *pole expansion*, inspired by PEXSI. We see that the same contour

integration technique as used in PEXSI can be applied to the *square-root* Fermi-Dirac function, after making a suitable choice of branch cut.

Notably, our theory only directly concerns the *Hartree approximation*, in which $v_{\text{hxc}} = v_{\text{h}}$ and the exchange and correlation components of v_{hxc} are neglected. From a chemical point of view, this is not considered an effective approximation in electronic structure theory. However, from an algorithmic point of view, we believe that our analysis is significant, because the Hartree contribution is typically dominant in absolute terms, and the algorithm itself generalizes easily. We offer a more detailed discussion of implications for more general DFT in Appendix D.

Concretely, the Hartree energy enables rigorous analysis because it is:

1. **Convex.** More general exchange-correlation functionals are not convex and can even admit many local optima, or self-consistent solutions of the Kohn-Sham equations, complicating the notion of ‘the’ physically correct solution.
2. **Quadratic.** The fact that the Hartree energy is quadratic will imply that our estimator for the Hartree potential is unbiased. Possibly, the impact of bias due to exchange-correlation contributions may be less important due to their smaller magnitude, but we leave further analysis of this possibility for future work.

In our analysis of the Hartree theory, we justify the somewhat surprising stylized conclusion that *solving the self-consistent Hartree theory from scratch is about as easy as estimating the Hartree energy for fixed ρ* . Under the hood, the idea supporting this conclusion is that the convergence rate of stochastic mirror descent (in which a single-shot estimator is used in each optimization step) balances perfectly with the slow Monte Carlo error rate for the stochastic estimator. To establish these claims, we need an analysis of stochastic mirror descent that explains the self-averaging in the effective potential that takes place over many iterations. Later in the introduction, we will review the broader context of mirror descent.

Before offering a more refined summary of our scaling results in terms of β and ε , we must distinguish two qualitatively different limits in which the basis set size n tends to infinity:

1. The **thermodynamic limit**. This limit is inspired by a scenario in which a basis set of uniform resolution is used to discretize an expanding volume, which in particular covers the case where a quantum chemistry basis set [33] of fixed accuracy is applied to an enlarging molecule. In particular, we view the discretization of the non-interacting Hamiltonian (including the Laplacian term) as bounded in this limit. Moreover, it is reasonable to assume (via Lemma 1) that a sort of gradient bound holds in this limit, as we argue via physical considerations in Section 6. Finally, the strong convexity parameter for the fermionic entropy (Lemma 2) can be viewed as proportional to the volume in this limit, which justifies the notion of relative energy error appearing in the main convergence theorem (Theorem 17).
2. The **complete basis set limit**. In this limit, we consider a basis set of increasingly fine resolution over a fixed volume. In this limit, as we have mentioned above, the pole expansion approach to discretizing the square-root Fermi-Dirac function becomes necessary to maintain optimal scaling. But, in addition, the analysis bounding the number of optimization iterations must also be adapted to this case. To avoid confining ourselves to an unnecessarily concrete choice of basis, we make certain assumptions on the eigenvalue growth of the non-interacting

Hamiltonian, which are intuitive due to the Laplacian term, and prove that this growth essentially confines the optimizer to a sector of constant dimension in which suitable strong convexity holds. Another subtle point is that an alternative initialization must be chosen for the mirror descent algorithm to avoid dependence on the spectral norm of the Laplacian. The main convergence results are given in Theorem 28 and Corollary 30. (Note that a suitable notion of relative energy error must be defined.)

Throughout, we attempt to keep the analysis as general as possible in terms of the basis set, preferring to identify physically reasonable assumptions, rather than fixate on establishing these assumptions for any particular choice of basis set.

Now we turn to a more refined summary of the scaling in terms of the error tolerance ε and the inverse temperature β . The additional factor due to error dependence is always $\tilde{O}(\varepsilon^{-2})$, but the factor due to temperature dependence is different in the two limits. Note also that our notion of energy error is a relative notion that is explained in further detail in the two main theorems (Theorems 17 and 28). Then in the thermodynamic limit, there is no additional dependence of the number of iterations on β . However, in the complete basis set limit, there is an additional factor of $\tilde{O}(\sqrt{\beta})$. Thus in the two limits, the overall scalings of the number of iterations are $\tilde{O}(\varepsilon^{-2})$ and $\tilde{O}(\sqrt{\beta} \varepsilon^{-2})$, respectively.

Next we turn to a discussion of the cost scaling of each iteration. For a general basis set of size n , we must also introduce an auxiliary grid of size m to spatially resolve the electron density ρ . We relate the grid to the basis set via a suitable factorization of the two-electron integrals known as tensor hypercontraction [15, 32, 16] and its interpretation as an interpolative separable density fitting [28], cf. Section 6.2. For the purpose of this summary, we have in mind the special case of the periodic sinc basis set used in our numerical experiments, for which $m = n$, and for which there is a direct correspondence between basis functions and grid points.

Now the dominant cost of each stochastic mirror descent iteration is the cost of a single matrix-vector multiplication by $f_{\beta}^{1/2}(H_{\text{eff}})$. For the purposes of our convergence results, we neglect the error δ of this approximation for simplicity. However, note that in the thermodynamic limit in which the effective Hamiltonian remains bounded, standard approximation theory results [34] guarantee that Chebyshev approximation suffices to achieve $\tilde{O}(\sqrt{\beta} \log(1/\delta) n)$ complexity for this task. In the complete basis set limit, heuristically one expects that a similar scaling is achieved via the pole expansion technique (as we confirm numerically in our experiments), but a rigorous analysis is stymied by the difficulty of analyzing preconditioned linear solvers for indefinite systems. Nevertheless, we comment that by reducing to the positive definite case (at the cost of squaring the condition number), we could use the analysis of the preconditioned conjugate gradient algorithm to achieve $\tilde{O}(\beta \log(1/\delta) n)$ complexity in the thermodynamic limit, which is still enough to achieve the optimal scaling in terms of n .

For most of our results, we assume a fixed chemical potential for simplicity, though in Section 7 we explain how the algorithm with fixed chemical potential can be wrapped within another algorithmic layer to determine the chemical potential, at the cost of an additional factor of $O(\varepsilon^{-1})$. It may be interesting to consider alternative primal-dual approaches for optimizing the Hartree potential and the chemical potential at the same time, though we expect that such an approach may introduce additional dependence on β in the analysis, and we leave such considerations to future work.

Finally, we validate our theoretical results through detailed numerical experiments in Section 9, which demonstrate the scalability of our pole-expansion-based algorithm in both limits to discretizations using over a million points.

Before offering an outline of the paper, we close the introduction with a review of mirror descent and how our work fits into this context. Mirror descent (MD) is a versatile first-order optimization method originally proposed by [31] for convex problems. It has since become a cornerstone in both online learning and stochastic optimization due to its ability to adapt to high-dimensional settings and different norm geometries. The algorithm can be viewed as being induced by the choice of a convex ‘Bregman potential,’ which induces a mirror map to a dual domain as its gradient. Many practical applications of mirror descent take place on the probability simplex and, to a lesser extent, its quantum generalization (the set of density operators). To our knowledge, our work is the first exploration of a practical scenario in which mirror descent is applied to the domain of *fermionic density matrices*. The suitable choice of Bregman potential in our context is the Fermi-Dirac operator entropy, and interestingly we establish a connection between mirror descent in this framework and the SCF that is commonly applied to solve DFT.

More specifically, we must consider a suitable notion of stochastic mirror descent, due to the use of a stochastic estimator for the gradient, and exploit self-averaging over the optimization trajectory, as mentioned above. This task requires us to establish a suitable sub-exponential concentration bound for our gradient estimator, which can be lifted to a suitable concentration bound for a martingale difference sequence appearing in the error analysis of mirror descent. Although we offer our own complete proof to meet the specifics of our needs, we note that the lifting step finds several analogies in the literature on stochastic mirror descent. Indeed, [30, 19] establishes high-probability bounds for stochastic mirror descent (SMD) and accelerated stochastic mirror descent with i.i.d unbiased gradient estimators and sub-Gaussian noise; [26] considers a more general framework of SMD with unbounded domains; [36] establishes a convergence rate for SMD with infinite noise variance; [20] considers stochastic gradient descent with heavy-tailed noise using the notion of sub-Weibull distributions; and [11] further uses this class of distributions to establish convergence rates for SMD with heavy-tailed martingale noise.

1.1 Outline

In Section 2, we present the formulation of the Hartree theory as a convex optimization problem over fermionic density matrices, as well as the physical interpretation of the terms appearing in the objective. We also explain the assumptions on these terms needed to yield a suitable notion of gradient bound, to be justified later in Section 6. In Section 3, we present the mirror descent framework for solving this optimization problem, including some analysis of the strong convexity of the Bregman potential. In Section 4, we complete the description of the algorithm by presenting the gradient estimator for an arbitrary Galerkin basis and proving a suitable concentration bound. We also explain the matrix function approximation details required to implement the gradient estimator practically. In Section 5, we present a convergence theorem for our algorithm which establishes optimal scaling in the thermodynamic limit. In Section 6, we return to discuss the structure of the energy term and the physical considerations justifying our abstract assumptions. This completes the ‘main narrative’ for the optimal scaling of our approach in the thermodynamic limit.

In the remaining sections, we consider several ornamentations. To wit, in Section 7 we explain how the algorithm can be used as a subroutine within an algorithm for determining the chemical potential if the electron number (not the chemical potential) is fixed *a priori*. In Section 8, we consider the complete basis set limit and explain how the dependence on the spectral norm of the non-interacting Hamiltonian can be removed by making assumptions on its eigenvalue growth and taking a suitable initialization.

In Section 9, we present numerical experiments validating our theoretical results and, moreover, demonstrating the almost-linear scaling of the algorithm (including the novel pole expansion approach) in both the thermodynamic and complete basis set limits for model problems. For concreteness, we comment that each of our largest experiments, which considered grids / basis sets of size $n \approx 10^6$, consumed only about 8 hours on a single GPU.

Finally, we outline the content of several supporting appendices which are referenced as needed in the main text. In Appendix A, we prove several facts about the Fermi-Dirac entropy. In Appendix B, we prove the sub-exponential concentration bound on the trace estimator. In Appendix C we give background, details, and theory supporting the construction of the pole expansion for the square-root Fermi-Dirac function via contour integration. In Appendix D, we review considerations for more general DFT beyond the Hartree theory and comment on the relevance of our results in this broader setting. In Appendix E we give proofs supporting the main results of Section 7 on chemical potential optimization. Finally, in Appendix F we give proofs supporting the main results of Section 8 on the convergence theory in the complete basis set limit.

1.2 Acknowledgments

This material is based on work supported by the Applied Mathematics Program of the US Department of Energy (DOE) Office of Advanced Scientific Computing Research under contract number DE-AC02-05CH11231 and by the U.S. Department of Energy, Office of Science, Accelerated Research in Quantum Computing Centers, Quantum Utility through Advanced Computational Quantum Algorithms, grant no. DE-SC0025572. M.L. was partially supported by a Sloan Research Fellowship. The authors gratefully acknowledge conversations with Xiao Liu and Ben Shpiro on stochastic DFT.

2 Preliminaries

We are interested in an optimization problem of the form

$$\begin{aligned} & \underset{X \in \mathbb{R}^{n \times n}}{\text{minimize}} && F_\beta(X) - \mu \text{Tr}[X] \\ & \text{subject to} && 0 \preceq X \preceq \mathbf{I}_n. \end{aligned} \tag{2.1}$$

We can view this problem as unconstrained because F_β will act as a barrier for the domain

$$\mathcal{X} := \{X : 0 \preceq X \preceq \mathbf{I}_n\}.$$

Here $\beta \in (0, +\infty]$ defines the *inverse temperature*, which can be taken to be $+\infty$ by suitably interpreting expressions below, unless indicated otherwise. Meanwhile, μ is called the *chemical potential* and can be viewed as a Lagrange multiplier for the trace constraint in the following alternative problem:

$$\begin{aligned} & \underset{X \in \mathbb{R}^{n \times n}}{\text{minimize}} && F_\beta(X) \\ & \text{subject to} && \text{Tr}[X] = N, \\ & && 0 \preceq X \preceq \mathbf{I}_n. \end{aligned} \tag{2.2}$$

We will discuss later how to solve this constrained problem, given an oracle for solving the unconstrained problem.

For context, we remark that in both problems, $X = (X_{ij})_{i,j=1}^n$ denotes the matrix of coefficients of the ***density matrix***

$$P_X(x, y) := \sum_{i,j=1}^n X_{ij} \psi_i(x) \psi_j(y)$$

in a fixed orthonormal ***quantum chemistry basis*** $\{\psi_i\}_{i=1}^n$ of functions on \mathbb{R}^d . (For concreteness we can take $d = 3$, though the choice does not affect most of the ensuing considerations directly.)

In terms of X we may also define the ***electron density***

$$\rho_X(x) = P_X(x, x).$$

Observe that by orthonormality

$$\int_{\mathbb{R}^d} \rho_X(x) dx = \text{Tr}[X].$$

Since the integral of the electron density can be interpreted as the total electron number of the ensemble, the value $N \in [0, n]$ denotes the ***electron number***, which need not be an integer.

We will view $\{\psi_i\}$ as a quantum chemistry basis for an extended quantum system. Intuitively, we can imagine that the number of basis functions per atom as being bounded by a constant, and we are considering a system of increasing volume / number of atoms in the limit $n \rightarrow \infty$. For now, we will maintain an abstract perspective that avoids discussion of the physical modeling considerations underlying our optimization problems, but we will return to these considerations below in Section 6. We will further comment on general DFT, beyond the Hartree approximation, in Appendix D.

The objective F_β is interpreted as a ***free energy*** defined by

$$F_\beta(X) := E(X) + \frac{1}{\beta} S_{\text{FD}}(X),$$

which, informally speaking, is bounded within a constant factor of the free energy density per unit volume.

Within the definition for the free energy, $E(X)$ denotes the ***energy*** function and $S_{\text{FD}}(X)$ denotes the ***Fermi-Dirac entropy***:

$$S_{\text{FD}}(X) = \text{Tr}[X \log X] + \text{Tr}[(\mathbf{I}_n - X) \log(\mathbf{I}_n - X)].$$

We can view the domain of the convex function S_{FD} as

$$\mathcal{X} := \{X \in \mathbb{R}^{n \times n} : 0 \preceq X \preceq \mathbf{I}_n\},$$

and the Fermi-Dirac entropy acts as a soft barrier for this domain.

Finally, the energy function $E(X)$ will take the form

$$E(X) = \text{Tr}[CX] + \tilde{E}(X),$$

where $C \in \mathbb{R}^{n \times n}$ is symmetric (and the notation is chosen by analogy to the usual notation for the linear cost term in semidefinite programming) and where

$$\tilde{E}(X) = \frac{1}{2} \sum_{ijkl} X_{ij} v_{ij,kl} X_{kl}$$

is the **Hartree energy**. The tensor $v_{ij,kl}$ will consist of the electron repulsion integrals (ERI).

We assume that

$$v_{ij,kl} = \sum_{p,q=1}^m \Psi_{pi} \Psi_{pj} V_{pq} \Psi_{qk} \Psi_{ql}, \quad (2.3)$$

where $\Psi = (\Psi_{pi}) \in \mathbb{R}^{m \times n}$ has orthonormal columns (i.e., satisfies $\Psi^\top \Psi = \mathbf{I}_n$) and $V = (V_{pq}) \in \mathbb{R}^{m \times m}$ is *positive semidefinite*. In particular it follows that $E(X)$ is *convex*.

In Section 6, we will explain the physical background and modeling conditions that support this structure for the energy function.

The key quantities appearing in our error analysis will be the spectral norm $\|C\|$ and the induced operator norm $\|V\|_\infty = \max_i \sum_j |V_{ij}|$, as well as the quantity

$$c_\Psi := \max_{p=1,\dots,m} \sum_{i=1}^n |\Psi_{pi}|^2. \quad (2.4)$$

We will also explain how these quantities are controlled in terms of the underlying physical problem in Section 6.2. In fact c_Ψ and $\|V\|_\infty$ appear together via their product, which we give its own notation:

$$c_h := c_\Psi \|V\|_\infty, \quad (2.5)$$

in which ‘h’ is for Hartree. To tackle the complete basis set limit, we will have to alter our perspective somewhat, and the relevant discussion is deferred to Section 8.

For now, it is useful to observe that the gradient of the quadratic term can be written

$$[\nabla \tilde{E}(X)]_{ij} = \sum_{kl} v_{ij,kl} X_{kl}.$$

Moreover, it is useful to define $\rho(X) = [\rho_q(X)]_{q=1}^m \in \mathbb{R}^m$ by

$$\rho_q(X) = \sum_{k,l=1}^n \Psi_{qk} X_{kl} \Psi_{ql}, \quad (2.6)$$

or alternatively as

$$\rho(X) = \text{diag} [\Psi X \Psi^\top]. \quad (2.7)$$

As we shall elucidate in Section 6.2, the vector $\rho_q(X)$ can be interpreted as the electron density $\rho_X(x_q)$ evaluated at a collection of interpolation points $\{x_q\}_{q=1}^m$.

In terms of $\rho(X)$, we can alternatively write $\tilde{E}(X)$ as a quadratic form:

$$\tilde{E}(X) = \frac{1}{2} \rho(X)^\top V \rho(X),$$

and we can also express $\nabla \tilde{E}(X)$ in terms of $\rho(X)$ as

$$\nabla \tilde{E}(X) = \Psi^\top \text{diag}^* [V \rho(X)] \Psi. \quad (2.8)$$

Here ‘diag*’ is the operator that returns a diagonal matrix with specified diagonal, which is the formal adjoint of the operator that returns the diagonal of a square matrix. We can identify $\nabla \tilde{E}(X)$ physically as the **Hartree potential**.

The importance of c_h owes to the following elementary lemma, which bounds the spectral norm of the gradient $\nabla \tilde{E}(X)$ (hence the notation ‘G’ for gradient). Together with a bound on $\|C\|$, this offers a bound on the spectral norm of $\nabla E(X) = C + \nabla \tilde{E}(X)$.

Lemma 1. *For any $Y \in \mathbb{R}^{n \times n}$, $\|\nabla \tilde{E}[Y]\| \leq c_h \|Y\|$, and $\|\rho(Y)\|_\infty \leq c_\Psi \|Y\|$.*

Proof. Note that by (2.8), since Ψ is an isometry it suffices to show that $\|V\rho(Y)\|_\infty \leq c_\Psi \|V\|_\infty \|Y\|$. In turn it suffices to show that $\|\rho(Y)\|_\infty \leq c_\Psi \|Y\|$.

To see this, note that by (2.6), we have

$$\rho_q(Y) = \langle \Psi_{q,:}, Y \Psi_{q,:} \rangle \leq \|\Psi_{q,:}\| \|Y \Psi_{q,:}\| \leq c_\Psi \|Y\|,$$

where we have used the definition (2.4) of c_Ψ . This completes the proof. \square

3 Mirror descent framework

Since (2.1) is a continuous optimization problem on a compact domain, we know that there exists a minimizer X_\star . (Moreover the minimizer is unique when $\beta < +\infty$ by strict convexity.)

We will solve the unconstrained problem (2.1) using mirror descent, induced by the choice of S_{FD} as our **Bregman potential** on \mathcal{X} . See [2] for a complete background on mirror descent. Here we highlight the structure of a few of the key objects that arises from this choice of Bregman potential.

First, the **mirror map** ∇S_{FD} defined by our choice is given by

$$\nabla S_{\text{FD}}(X) = \log(X(\mathbf{I}_n - X)^{-1}),$$

and the convex conjugate S_{FD}^* of the Bregman potential is defined by

$$S_{\text{FD}}^*(X^*) = \text{Tr} \left[\log(\mathbf{I}_n + e^{X^*}) \right].$$

The domain \mathcal{X}^* of S_{FD}^* is the set of all symmetric $n \times n$ matrices. The gradient of the convex conjugate S_{FD}^* defines the **inverse mirror map**:

$$\nabla S_{\text{FD}}^*(X^*) = (\mathbf{I}_n + e^{-X^*})^{-1}.$$

The Bregman potential also fixes a **Bregman divergence**:

$$D(Y\|X) := S_{\text{FD}}(Y) - S_{\text{FD}}(X) - \langle \nabla S_{\text{FD}}(X), Y - X \rangle$$

for $X, Y \in \mathcal{X}$. (Here and throughout the manuscript, $\langle \cdot, \cdot \rangle$ refers to the Frobenius inner product.)

3.1 Algorithm overview

The mirror descent iteration ((2.7) in [2]) (with step size $\gamma_t > 0$ at iteration t) for (2.1) is defined by

$$\nabla S_{\text{FD}}(X_{t+1}) = (1 - \beta^{-1}\gamma_t)\nabla S_{\text{FD}}(X_t) - \gamma_t(\nabla E(X_t) - \mu\mathbf{I}_n).$$

We will offer a more physical interpretation in Section 3.2 below. For reasons to be clarified in Section 3.3, due to an alternative interpretation of this algorithm, we will always take $\gamma_t \leq \beta$.

As we shall see later, computational efficiency demands that we estimate ∇E stochastically. For this reason, we are interested more generally in the approximate update

$$\nabla S_{\text{FD}}(X_{t+1}) = (1 - \beta^{-1}\gamma_t)\nabla S_{\text{FD}}(X_t) - \gamma_t(G_t - \mu\mathbf{I}_n), \quad (3.1)$$

where G_t is an estimator for the gradient.

As our initial condition we take

$$X_0 = \frac{1}{2}\mathbf{I}_n,$$

and we let T denote the time horizon of the algorithm, which furnishes iterates X_0, \dots, X_T . (We will consider an alternative initial condition in Section 8.)

In Section 4 we will explain how the gradient estimator is constructed and how several key properties are guaranteed.

3.2 Physical interpretation ($\beta < +\infty$)

In this section we assume $\beta < +\infty$.

It is useful to define the *Fermi-Dirac function*

$$f_\beta(x) = \frac{1}{1 + e^{\beta x}}.$$

Then evidently

$$\nabla S_{\text{FD}}^*(X^*) = f_\beta(-\beta^{-1}X^*) = f_\beta(H),$$

where we view $H := -\beta^{-1}X^*$ as an *effective Hamiltonian* corresponding to our state $X \in \mathcal{X}$, corresponding to $X^* \in \mathcal{X}^*$ via the mirror map.

If we define

$$H_t = -\beta^{-1}X_t^* = -\beta^{-1}\nabla S(X_t), \quad t = 1, \dots, T,$$

then we can alternatively characterize the mirror descent update (3.1) as an update rule for the effective Hamiltonian:

$$H_{t+1} = (1 - \beta^{-1}\gamma_t)H_t + \beta^{-1}\gamma_t(G_t - \mu\mathbf{I}_n), \quad (3.2)$$

where $H_0 = 0$. In each update we set H_{t+1} to be a convex combination of the H_t with $G_t - \mu\mathbf{I}_n$.

Notice that any fixed point of the iteration map in which exact gradients $G_t = \nabla E(X_t)$ are used (which necessarily coincides with the unique optimizer X_\star) must satisfy

$$H_\star = \nabla E(X_\star) - \mu\mathbf{I}_n, \quad X_\star = f_\beta(\nabla E(X_\star) - \mu\mathbf{I}_n). \quad (3.3)$$

3.3 Formulation as a proximal algorithm

We introduced the update (3.1) as the instantiation of mirror descent on the objective

$$E(X) - \mu \text{Tr}[X] + \beta^{-1}S_{\text{FD}}(X)$$

with Bregman potential S_{FD} and step size $\gamma_t > 0$. However, we can equivalently view the same update as a proximal algorithm:

$$X_{t+1} = \underset{X \in \mathcal{X}}{\operatorname{argmin}} \left\{ E(X_t) + \langle G_t - \mu \mathbf{I}_n, X - X_t \rangle + \frac{1}{\beta} S_{\text{FD}}(X) + \frac{1}{\eta_t} D(X \| X_t) \right\}, \quad (3.4)$$

for a certain choice of $\eta_t > 0$.

Note that mirror descent can *always* be interpreted as a proximal algorithm (Proposition 3.2 in [2]), but a key difference here is that the regularization term $\beta^{-1} S_{\text{FD}}(X)$ is not linearized inside the ‘argmin.’ We are treating it exactly within the argmin in the sense of composite function minimization that is famously used for nonsmooth terms that enjoy exploitable structure [3]. Therefore this proximal formulation is different from the one that is automatically enjoyed by the update as an instance of mirror descent.

Now to establish the connection between (3.1) and (3.4), observe that solving the first-order optimality condition for (3.4) yields

$$\nabla S_{\text{FD}}(X_{t+1}) = \left(1 - \frac{\eta_t}{\eta_t + \beta} \right) \nabla S(X_t) - \frac{\eta_t \beta}{\eta_t + \beta} (G_t - \mu \mathbf{I}_n),$$

which coincides with (3.1) under the identification

$$\gamma_t := \frac{\eta_t \beta}{\eta_t + \beta} < \beta.$$

3.4 Elementary facts

For now we state a key property of the Fermi-Dirac entropy, which follows from the famous strong convexity of the von Neumann entropy [5].

Lemma 2. S_{FD} is $(2/n)$ -strongly convex on \mathcal{X} with respect to the nuclear norm $\| \cdot \|_*$.

The proof is given in Appendix A.

It is also useful to show that the Bregman divergence from the initial condition $X_0 = \frac{1}{2} \mathbf{I}_n$ is bounded.

Lemma 3. For all $X \in \mathcal{X}$, we have

$$D(X \| X_0) \leq n \log 2.$$

The proof is also given in Appendix A.

4 Gradient estimator

An estimator for $\nabla \tilde{E}(X_t)$ can be defined by using a stochastic trace estimator [17] to estimate the density $\rho(X_t)$, viewed as a matrix diagonal following (2.7). Note that a similar estimator was used recently in [24], which also considered randomized algorithms for semidefinite programming. Remarkably, we will require only a single shot per optimization step in our estimator.

Indeed, let $z_0, \dots, z_{T-1} \in \mathbb{R}^n$ denote independent and identically distributed standard Gaussian random vectors. Then define

$$\hat{X}_t := X_t^{1/2} z_t z_t^\top X_t^{1/2} = \left[X_t^{1/2} z_t \right] \left[X_t^{1/2} z_t \right]^\top.$$

Note that the matrix square root $X_t^{1/2}$ can be viewed as a matrix function of H_t :

$$X_t^{1/2} = f_\beta^{1/2}(H_t),$$

where $\beta < +\infty$ for simplicity and $f_\beta^{1/2}$ is the pointwise square root of the Fermi-Dirac function. We will discuss below in Section 4.3 how this allows us to construct the matrix-vector multiplication $X_t^{1/2} z_t$ efficiently, without forming the matrix $X_t^{1/2}$ directly. For now we simply assume that this operation can be performed exactly.

Then define

$$\hat{\rho}_t := \rho(\hat{X}_t) = \text{diag} \left[\Psi \hat{X}_t \Psi^\top \right] = (\Psi X_t^{1/2} z_t)^{\odot 2}, \quad (4.1)$$

where the superscript denotes an entrywise power, and finally:

$$\tilde{G}_t := \nabla \tilde{E}(\hat{X}_t) = \Psi^\top \text{diag}^* [V \hat{\rho}_t] \Psi, \quad (4.2)$$

following the expression (2.8) for $\nabla \tilde{E}(X)$ in terms of $\rho(X)$.

It is useful to define the filtration $\{\mathcal{F}_t\}_{t=0}^{T-1}$ generated by the random vectors $\{z_t\}_{t=0}^{T-1}$. Then evidently X_{t+1} is measurable with respect to \mathcal{F}_t for $t = 0, \dots, T-1$, and moreover

$$\begin{aligned} \mathbb{E}[\hat{X}_t \mid \mathcal{F}_{t-1}] &= X_t, \\ \mathbb{E}[\hat{\rho}_t \mid \mathcal{F}_{t-1}] &= \rho(X_t), \\ \mathbb{E}[\tilde{G}_t \mid \mathcal{F}_{t-1}] &= \nabla \tilde{E}(X_t). \end{aligned}$$

In particular, \tilde{G}_t defines an unbiased estimator for the gradient at step t (conditioned on the previous randomness).

We finally define our full gradient estimate as

$$G_t = C + \tilde{G}_t, \quad (4.3)$$

which satisfies

$$\mathbb{E}[G_t \mid \mathcal{F}_{t-1}] = \nabla E(X_t).$$

It is also useful to define the error of the estimator:

$$\Delta_t := G_t - \nabla E(X_t) = \tilde{G}_t - \nabla \tilde{E}(X_t), \quad (4.4)$$

which satisfies

$$\mathbb{E}[\Delta_t \mid \mathcal{F}_{t-1}] = 0.$$

4.1 Sub-exponential concentration

We need concentration bounds for quantities related to the gradient estimator. To formulate these, we state the definition of a sub-exponential random variable, following the text of [37]. (We will use lower-case letters to denote scalar random variables and vectors in this manuscript, in order to avoid confusion with the capital-letter notation for matrices.) We slightly extend definitions to deal with the fact that our sequence of iterates X_t is random, while at each iteration the random vector z_t is chosen independently of all preceding randomness.

Definition 4 (Definition 2.7 of [37]). A random variable x with mean $\mu = \mathbb{E}[x]$ is sub-exponential if there are non-negative parameters (ν, b) such that

$$\mathbb{E} \left[e^{\lambda(x-\mu)} \right] \leq e^{\frac{\nu^2 \lambda^2}{2}} \quad \text{for all } |\lambda| \leq \frac{1}{b}.$$

Given a σ -algebra \mathcal{F} , we will say that x satisfying $\mu = \mathbb{E}[x | \mathcal{F}]$ is sub-exponential with parameters (ν, b) , *conditioned on \mathcal{F}* , if

$$\mathbb{E} \left[e^{\lambda(x-\mu)} | \mathcal{F} \right] \leq e^{\frac{\nu^2 \lambda^2}{2}} \quad \text{for all } |\lambda| \leq \frac{1}{b}$$

holds almost surely. Here $\nu, b \geq 0$ can be random variables which are measurable with respect to \mathcal{F} .

Importantly, sub-exponential random variables satisfy the following tail bound, which we adapt from [37]:

Proposition 5 (Proposition 2.9 of [37]). *Suppose that x is sub-exponential with parameters (ν, b) and $\mathbb{E}[x] = \mu$. Then for $t \geq 0$,*

$$\mathbb{P} [x \geq \mu + t] \leq \begin{cases} e^{-\frac{t^2}{2\nu^2}}, & \text{if } 0 \leq t \leq \frac{\nu^2}{b}, \\ e^{-\frac{t}{2b}}, & \text{if } t > \frac{\nu^2}{b}. \end{cases}$$

Likewise, if x is sub-exponential with parameters (ν, b) , conditioned on some σ -algebra \mathcal{F} , and $\mathbb{E}[x | \mathcal{F}] = \mu$, then for $t \geq 0$, it holds almost surely that

$$\mathbb{P} [x \geq \mu + t | \mathcal{F}] \leq \begin{cases} e^{-\frac{t^2}{2\nu^2}}, & \text{if } 0 \leq t \leq \frac{\nu^2}{b}, \\ e^{-\frac{t}{2b}}, & \text{if } t > \frac{\nu^2}{b}. \end{cases}$$

Remark 6. The second statement can be proved just by following the ordinary proof of the first statement, which uses the Chernoff technique. But we can also view the second statement as following directly from the first statement via the regular conditional probability.

In order to state some results more transparently later on, we state and prove the following simple corollary.

Corollary 7. *Suppose x is sub-exponential with deterministic parameters $(\nu, 2\nu)$, conditioned on some σ -algebra \mathcal{F} , and $\mathbb{E}[x | \mathcal{F}] = \mu$. Then for any $\delta \in (0, 1]$,*

$$x \leq \mu + \nu \left(\frac{1}{2} + 4 \log(1/\delta) \right)$$

with probability at least $1 - \delta$.

The proof is given in Appendix B.

Sub-exponential concentration bounds are relevant because if $z \sim \mathcal{N}(0, \mathbf{I}_n)$, the trace estimator $z^\top A z$, which satisfies $\mathbb{E}[z^\top A z] = \text{Tr}[A]$, is a sub-exponential random variable. The result is true more generally the entries of z are i.i.d. sub-Gaussian random variables with zero mean and unit variance [29]. However, for simplicity, we just consider the case of Gaussian z and extend the usual statement to account for the fact that the matrix A may be random, while z is chosen independently of A .

Lemma 8. *Let \mathcal{F} be a σ -algebra, and let $A \in \mathbb{R}^{n \times n}$ be a random matrix that is measurable with respect to \mathcal{F} . Let $z \sim \mathcal{N}(0, \mathbf{I}_n)$ be independent of \mathcal{F} . Then $z^\top A z$ is sub-exponential with parameters $(2\|A\|_F, 4\|A\|)$, conditioned on \mathcal{F} .*

The proof is also given in Appendix B.

We will need one more definition and result from [37]:

Definition 9 ((2.26) of [37]). We say that a sequence $\{y_t\}_{t=0}^{T-1}$, adapted to the filtration $\{\mathcal{F}_t\}_{t=0}^{T-1}$, is a *martingale difference sequence* if $\mathbb{E}[y_t] < +\infty$ for all $t = 0, \dots, T-1$ and

$$\mathbb{E}[y_t | \mathcal{F}_{t-1}] = 0$$

for all $t = 1, \dots, T-1$.

Martingale difference sequences satisfy the following Bernstein-type concentration bound:

Theorem 10 (Theorem 2.19 of [37]). *Let $\{y_t\}_{t=0}^{T-1}$ be a martingale difference sequence adapted to the filtration $\{\mathcal{F}_t\}_{t=0}^{T-1}$, and suppose that y_t is sub-exponential with deterministic parameters (ν_t, b_t) , conditioned on \mathcal{F}_{t-1} . Then $\sum_{t=0}^{T-1} y_t$ is sub-exponential with parameters*

$$\left(\sqrt{\sum_{t=0}^{T-1} \nu_t^2}, \max_{t=0, \dots, T-1} \{b_t\} \right).$$

4.2 Gradient concentration bounds

We can apply Lemma 8 in several ways to obtain the following concentration bounds which will be used to control the convergence rate of (3.1) with high probability.

The first is a bound on the spectral norm of the gradient.

Lemma 11. *For any $\delta \in (0, 1]$, the inequality*

$$\max_{t=0, \dots, T-1} \|\hat{G}_t\| \leq 2(1 + 4 \log(Tm/\delta)) c_h$$

holds with probability at least $1 - \delta$.

Proof. Note that each entry of $\hat{\rho}_t = \text{diag}[\Psi \hat{X}_t \Psi^\top]$ (cf. (4.1)) can be viewed as a trace estimate via

$$[\hat{\rho}_t]_q = z_t^\top \left[X_t^{1/2} \Psi^\top e_q e_q^\top \Psi X_t^{1/2} \right] z_t.$$

Hence by Lemma 8, for $t \geq 1$ the random variable $[\hat{\rho}_t]_q$ is sub-exponential with parameters $(2\|A_t\|_F, 4\|A_t\|)$, conditioned on \mathcal{F}_{t-1} , where $A_t := X_t^{1/2}\Psi^\top e_q e_q^\top \Psi X_t^{1/2}$. (When $t = 0$, A_t is deterministic, so $\hat{\rho}_1$ is simply sub-exponential with these parameters.)

This matrix A_t is rank-one and we can compute $\|A_t\|_F = \|A_t\| = \sqrt{\text{Tr}[A_t^2]} = [\rho(X_t)]_q$. From Lemma 1, we have that $\|\rho(X_t)\|_\infty \leq c_\Psi \|X_t\| \leq c_\Psi$. Therefore each entry $[\hat{\rho}_t]_q$ is sub-exponential with the deterministic parameters $(2c_\Psi, 4c_\Psi)$, conditioned on \mathcal{F}_{t-1} . (Again, we don't need to condition for $t = 0$.)

We can then apply Corollary 7 with $\nu = 2c_\Psi$ to deduce that

$$[\hat{\rho}_t]_q \leq [\rho(X_t)]_q + c_\Psi (1 + 8 \log(Tm/\delta))$$

holds with probability at least $1 - \frac{\delta}{Tm}$.

Then by the union bound, together with the fact that $[\rho(X_t)]_q \leq \|\rho(X_t)\|_\infty \leq c_\Psi$, we conclude that

$$\|\hat{\rho}_t\|_\infty \leq 2(1 + 4 \log(Tm/\delta)) c_\Psi$$

holds for all $t = 0, \dots, T-1$ with probability at least $1 - \delta$.

Then it follows that

$$\|\hat{G}_t\| = \|\Psi^\top \text{diag}^*[V\hat{\rho}_t]\Psi\| \leq \|V\|_\infty \|\hat{\rho}_t\|_\infty \leq 2(1 + 4 \log(Tm/\delta)) c_h$$

holds for all $t = 0, \dots, T-1$ with probability at least $1 - \delta$, as was to be shown. \square

Next is a fact that we will need in combination with Theorem 10 above.

Lemma 12. *Suppose $Y \in \mathbb{R}^{n \times n}$ is random but measurable with respect to \mathcal{F}_{t-1} for some $t \geq 1$, and define $y = \langle \Delta_t, Y \rangle$. Assume that $\|Y\| \leq 1$. Then y is sub-exponential with parameters $(2c_h\|X_t\|_F, 4c_h)$, conditioned on \mathcal{F}_{t-1} .*

Proof. Compute

$$\begin{aligned} \langle \tilde{G}_t, Y \rangle &= \langle \nabla \tilde{E}(\hat{X}_t), Y \rangle \\ &= \sum_{ijkl} Y_{ij} v_{ij,kl} [\hat{X}_t]_{kl} \\ &= \langle \hat{X}_t, \nabla \tilde{E}(Y) \rangle \\ &= \langle X_t^{1/2} z_t z_t^\top X_t^{1/2}, \nabla \tilde{E}(Y) \rangle \\ &= z_t^\top [X_t^{1/2} \nabla \tilde{E}(Y) X_t^{1/2}] z_t, \end{aligned}$$

so $\langle \tilde{G}_t, Y \rangle$ can be viewed as a trace estimator for $A := X_t^{1/2} \nabla \tilde{E}(Y) X_t^{1/2}$ (which is itself measurable with respect to \mathcal{F}_{t-1}). Then by Lemma 8, we have that $\langle \tilde{G}_t, Y \rangle$ is sub-exponential with parameters $(2\|A\|_F, 4\|A\|)$, conditioned on \mathcal{F}_{t-1} .

Since Y is measurable with respect to \mathcal{F}_{t-1} , we have that

$$\mathbb{E} [\langle \tilde{G}_t, Y \rangle \mid \mathcal{F}_{t-1}] = \langle \nabla \tilde{E}(X_t), Y \rangle,$$

and therefore

$$y = \langle \tilde{G}_t, Y \rangle - \mathbb{E} \left[\langle \tilde{G}_t, Y \rangle \mid \mathcal{F}_{t-1} \right],$$

i.e., y is the difference of $\langle \tilde{G}_t, Y \rangle$ and its conditional mean. It follows that y is sub-exponential with the same parameters, conditioned on \mathcal{F}_{t-1} .

Now we can compute

$$\|A\| = \|X_t^{1/2} \nabla \tilde{E}(Y) X_t^{1/2}\| \leq \|X_t^{1/2}\|^2 \|\nabla \tilde{E}(Y)\| \leq c_h,$$

where we have used Lemma 1 and the fact that $\|X_t\| \leq 1$ in the last inequality.

Moreover,

$$\begin{aligned} \|A\|_{\mathbb{F}}^2 &= \text{Tr} \left[\nabla \tilde{E}(Y) X_t \nabla \tilde{E}(Y) X_t \right] \\ &= \left\langle \left(\nabla \tilde{E}(Y) X_t \right)^\top, \nabla \tilde{E}(Y) X_t \right\rangle \\ &\leq \|\nabla \tilde{E}(Y) X_t\|_{\mathbb{F}}^2 \\ &\leq \|\nabla \tilde{E}(Y)\|^2 \|X_t\|_{\mathbb{F}}^2 \\ &\leq c_h^2 \|X_t\|_{\mathbb{F}}^2, \end{aligned}$$

and this completes the proof. \square

4.3 Matrix function implementation

In order to implement the gradient estimator we must perform the matrix-vector multiplications $X_t^{1/2} z_t$ within the construction of $\hat{\rho}_t$ (4.1). We already commented that when $\beta < +\infty$, we can think of

$$X_t^{1/2} = f_\beta^{1/2}(H_t) = f_1^{1/2}(\beta H_t).$$

One standard approach to such a matrix-vector multiplication involving a matrix function is to perform Chebyshev approximation [34] of order r of $f_\beta^{1/2}$ on an interval that bounds the spectrum of H_t . (Equivalently, we can perform Chebyshev approximation of $f_1^{1/2}$ on an interval bounding the spectrum of βH_t .) Then the three-term recurrence [34] can be used to compute $f_\beta^{1/2}(H_t) z_t$ using r matrix-vector multiplications by H_t , which we can construct efficiently.

Another approach involves the approximation of $f_\beta^{1/2}$ using a contour integral approach. A similar approach for approximating the Fermi-Dirac function is applied within PEXSI method [23, 22, 21] for DFT, but here we must adapt the approach to deal with the branch cut due to the square root. Ultimately, this approach requires us to solve several linear systems involving shifted copies of the effective Hamiltonian. The details are given in Appendix C.

We will not consider the error due to matrix function approximation in our ensuing analysis as it can be made exponentially small by increasing the polynomial order (in the first approach) or the number of poles (in the second approach). However, we comment that the second approach can benefit from a good preconditioner, which is particularly useful when a larger basis set is used and the norm of the discretized Laplacian operator appearing within H_t contributes to the conditioning.

Either approach motivates us to bound the spectrum of H_t over the optimization trajectory. This can be done in terms of the following bound for the gradient over the optimization trajectory.

Definition 13. Let

$$\tilde{g}_{\max} = \max_{t=0, \dots, T-1} \|\tilde{G}_t\|.$$

Remark 14. Recall from Lemma 11 that $\hat{g}_{\max} = O(c_h \log(Tm/\delta))$ with probability at least $1 - \delta$.

Lemma 15. Assume $\beta < +\infty$, fix T , and assume that $\gamma_t \in (0, \beta]$ for all $t = 0, \dots, T-1$. Then

$$\|H_t\| \leq \|C - \mu \mathbf{I}_n\| + \tilde{g}_{\max}$$

for all $t = 0, \dots, T$.

Proof. From (3.2) we know that the effective Hamiltonian satisfies the update

$$H_{t+1} = (1 - \beta^{-1}\gamma_t)H_t + (\beta^{-1}\gamma_t)(G_t - \mu \mathbf{I}_n).$$

Moreover, $G_t = C + \tilde{G}_t$, so

$$\|H_{t+1}\| \leq (1 - \beta^{-1}\gamma_t)\|H_t\| + (\beta^{-1}\gamma_t)(\|C - \mu \mathbf{I}_n\| + \tilde{g}_{\max})$$

for all $t = 0, \dots, T-1$.

Then by induction (noting that $H_0 = 0$) it follows that

$$\|H_t\| \leq \|C - \mu \mathbf{I}_n\| + \tilde{g}_{\max}$$

for all $t = 0, \dots, T$. □

5 Convergence theorem and proof

Now we prove the convergence of the algorithm (3.1). For the proof, we are inspired by [2], from which we adapt several key facts and arguments. In particular, we reproduce the statement of this lemma (Lemma 2 from [6]):

Lemma 16. Let Φ be convex on \mathcal{X} , $\tilde{X} \in \mathcal{X}$, and

$$X' = \operatorname{argmin}_{X \in \mathcal{X}} \left\{ \Phi(X) + D(X\|\tilde{X}) \right\}.$$

Then for any $Y \in \mathcal{X}$, we have

$$\Phi(Y) + D(Y\|\tilde{X}) \geq \Phi(X') + D(X'\|\tilde{X}) + D(Y\|X').$$

Now we state and prove our convergence theorem.

Theorem 17. For any $\delta \in (0, 1]$, define $c_{T,m,\delta} := 2(1 + 4\log(2Tm/\delta))$. Consider algorithm defined by (3.4) with step size $\eta_t = \eta := \frac{1}{c_{T,m,\delta} c_h \sqrt{T}}$, or equivalently by (3.1) with $\gamma_t := \frac{\eta\beta}{\eta+\beta}$, and initial condition $X_0 = \mathbf{I}_n/2$. Then

$$\frac{1}{T} \sum_{t=0}^{T-1} \frac{F_\beta(X_t) - \mu \operatorname{Tr}[X_t]}{n} \leq \frac{F_\beta(X_\star) - \mu \operatorname{Tr}[X_\star]}{n} + \frac{c_{T,m,\delta} c_h}{\sqrt{T}} \left(\log 2 + \frac{1}{4} + \frac{1}{\sqrt{n}} \right) + \frac{\|C - \mu \mathbf{I}_n\|}{T}$$

holds with probability at least $1 - \delta$.

Remark 18. In particular it follows that there exists $t \in \{0, 1, \dots, T-1\}$ such that

$$\frac{F_\beta(X_t) - \mu \text{Tr}[X_t]}{n} \leq \frac{F_\beta(X_\star) - \mu \text{Tr}[X_\star]}{n} + O\left(\frac{c_h \log(Tm/\delta)}{\sqrt{T}}\right) + \frac{\|C - \mu \mathbf{I}_n\|}{T}.$$

It also follows from the theorem, by the convexity of F_β , that

$$\frac{F_\beta(\bar{X}_T) - \mu \text{Tr}[\bar{X}_T]}{n} \leq \frac{F_\beta(X_\star) - \mu \text{Tr}[X_\star]}{n} + O\left(\frac{c_h \log(Tm/\delta)}{\sqrt{T}}\right) + \frac{\|C - \mu \mathbf{I}_n\|}{T},$$

where $\bar{X}_T := \frac{1}{T} \sum_{t=0}^{T-1} X_t$ is the Cesàro sum.

Remark 19. It is sensible to expect that the error bound for the objective should scale with n , since the optimal value itself should scale at least size-extensively as $\Omega(n)$. In fact, it may even scale faster, due to the heavy tails of the electron-electron Coulomb interaction, as we shall discuss below in Section 6.2. We can view $\frac{1}{n}F_\beta$ as the **free energy density** per basis function.

Remark 20. Observe that the dependence of the error on $\|C - \mu \mathbf{I}_n\|$ (which is modulated by $1/T$) is milder than the dependence on c_h (which is modulated by $1/\sqrt{T}$). This is fortunate because in our intended applications, C involves the Galerkin projection of a Laplacian operator, which may have a significantly larger norm than c_h (which arises from the discretization of an integral operator). In practice, however, quantum chemistry basis sets are not so large that $\|C\|$ should be considered unbounded.

Proof. For simplicity, without loss of generality we can set $\mu = 0$ by absorbing $\mu \text{Tr}[X]$ into the definition of $E(X)$ via the replacement $C \leftarrow C - \mu \mathbf{I}_n$.

Recall $G_t = C + \tilde{G}_t$ denotes our gradient estimator (4.3), where \tilde{G}_t is defined by (4.2). Also recall that $\Delta_t = G_t - \nabla E(X_t)$ denotes the error of our gradient estimator (defined earlier in (4.4)), and that $\mathbb{E}[\Delta_t | \mathcal{F}_{t-1}] = 0$.

Within Lemma 16, consider the choice

$$\Phi(X) = \eta \left[E(X_t) + \langle G_t, X - X_t \rangle + \frac{1}{\beta} S_{\text{FD}}(X) \right],$$

for Φ . Also consider X_t in the place of \tilde{X} , as well as X_\star in the place of Y . Our proximal interpretation of the update (3.4) indicates that moreover we can take X_{t+1} in the place of X' . Then we deduce

$$\begin{aligned} & \eta \left[E(X_t) + \langle G_t, X_\star - X_t \rangle + \frac{1}{\beta} S_{\text{FD}}(X_\star) \right] + D(X_\star \| X_t) \\ & \geq \eta \left[E(X_t) + \langle G_t, X_{t+1} - X_t \rangle + \frac{1}{\beta} S_{\text{FD}}(X_{t+1}) \right] + D(X_{t+1} \| X_t) + D(X_\star \| X_{t+1}). \end{aligned}$$

We can then cancel and rearrange terms to determine that

$$D(X_\star \| X_{t+1}) \leq D(X_\star \| X_t) + \eta \langle G_t, X_\star - X_{t+1} \rangle + \frac{\eta}{\beta} [S_{\text{FD}}(X_\star) - S_{\text{FD}}(X_{t+1})] - D(X_{t+1} \| X_t). \quad (5.1)$$

Now the strong convexity of S_{FD} (Lemma 2) implies that

$$D(X_{t+1} \| X_t) \geq \frac{1}{n} \|X_{t+1} - X_t\|_*^2, \quad (5.2)$$

and we can also compute

$$\begin{aligned}
\langle G_t, X_\star - X_{t+1} \rangle &= \langle G_t, X_\star - X_t \rangle + \langle G_t, X_t - X_{t+1} \rangle \\
&= \langle \nabla E(X_t), X_\star - X_t \rangle + \langle \Delta_t, X_\star - X_t \rangle + \langle G_t, X_t - X_{t+1} \rangle \\
&= \langle \nabla E(X_t), X_\star - X_t \rangle + \langle \Delta_t, X_\star - X_t \rangle + \langle C, X_t - X_{t+1} \rangle + \left\langle \tilde{G}_t, X_t - X_{t+1} \right\rangle \\
&\leq [E(X_\star) - E(X_t)] + \langle \Delta_t, X_\star - X_t \rangle + \langle C, X_t - X_{t+1} \rangle + \|\tilde{G}_t\| \|X_{t+1} - X_t\|_*,
\end{aligned} \tag{5.3}$$

where in the last line we have used the convexity of E and the fact that the spectral and nuclear norms are duals.

Then by combining (5.1), (5.2), and (5.3), we obtain:

$$\begin{aligned}
D(X_\star \| X_{t+1}) &\leq D(X_\star \| X_t) + \eta [E(X_\star) - E(X_t)] + \eta \langle \Delta_t, X_\star - X_t \rangle + \frac{\eta}{\beta} [S_{\text{FD}}(X_\star) - S_{\text{FD}}(X_{t+1})] \\
&\quad + \eta \langle C, X_t - X_{t+1} \rangle + \eta \|\tilde{G}_t\| \|X_{t+1} - X_t\|_* - \frac{1}{n} \|X_{t+1} - X_t\|_*^2.
\end{aligned} \tag{5.4}$$

Now we can use the general inequality $ab \leq \frac{1}{2}a^2 + \frac{1}{2}b^2$ to bound the first expression in the last line:

$$\eta \|\tilde{G}_t\| \|X_{t+1} - X_t\|_* \leq \frac{n}{4} \eta^2 \|\tilde{G}_t\|^2 + \frac{1}{n} \|X_{t+1} - X_t\|_*^2. \tag{5.5}$$

Then combining (5.4) and (5.5) and defining $d_t := D(X_\star \| X_t)$ for all t , we find that

$$\begin{aligned}
d_{t+1} - d_t &\leq \eta [E(X_\star) - E(X_t)] + \eta \langle \Delta_t, X_\star - X_t \rangle + \frac{\eta}{\beta} [S_{\text{FD}}(X_\star) - S_{\text{FD}}(X_{t+1})] \\
&\quad + \eta \langle C, X_t - X_{t+1} \rangle + \frac{n}{4} \eta^2 \|\tilde{G}_t\|^2.
\end{aligned}$$

Now recall that $F_\beta = E + \beta^{-1} S_{\text{FD}}$, so we can group terms to obtain

$$\begin{aligned}
d_{t+1} - d_t &\leq \eta [F_\beta(X_\star) - F_\beta(X_t)] + \eta \langle \Delta_t, X_\star - X_t \rangle + \frac{\eta}{\beta} [S_{\text{FD}}(X_t) - S_{\text{FD}}(X_{t+1})] \\
&\quad + \eta \langle C, X_t - X_{t+1} \rangle + \frac{n}{4} \eta^2 \|\tilde{G}_t\|^2
\end{aligned}$$

and, after some further rearrangement to isolate the terms involving F_β :

$$\begin{aligned}
[F_\beta(X_t) - F_\beta(X_\star)] &\leq \frac{1}{\eta} [d_t - d_{t+1}] + \frac{n}{4} \eta \|\tilde{G}_t\|^2 + \langle \Delta_t, X_\star - X_t \rangle \\
&\quad + \langle C, X_t - X_{t+1} \rangle + \frac{1}{\beta} [S_{\text{FD}}(X_t) - S_{\text{FD}}(X_{t+1})].
\end{aligned}$$

Finally we can sum both sides over $t = 0, \dots, T-1$, taking advantage of telescoping, to deduce:

$$\begin{aligned}
\sum_{t=0}^{T-1} [F_\beta(X_t) - F_\beta(X_\star)] &\leq \frac{1}{\eta} [d_0 - d_T] + \frac{n}{4} \eta \sum_{t=0}^{T-1} \|\tilde{G}_t\|^2 + \sum_{t=0}^{T-1} \langle \Delta_t, X_\star - X_t \rangle \\
&\quad + \langle C, X_0 - X_T \rangle + \frac{1}{\beta} [S_{\text{FD}}(X_0) - S_{\text{FD}}(X_T)].
\end{aligned} \tag{5.6}$$

Note that our initialization $X_0 = \mathbf{I}_n/2$ was chosen to minimize S_{FD} , the last expression on the right-hand side is ≤ 0 . Moreover $d_T \geq 0$, and $\langle C, X_0 - X_T \rangle \leq \|C\| \|X_0 - X_T\|_* \leq n\|C\|$ (since $-\mathbf{I}_n \preceq X_0 - X_T \preceq \mathbf{I}_n$), so we obtain a simpler inequality:

$$\sum_{t=0}^{T-1} [F_\beta(X_t) - F_\beta(X_*)] \leq \frac{d_0}{\eta} + \frac{n}{4}\eta \sum_{t=0}^{T-1} \|\tilde{G}_t\|^2 + \sum_{t=0}^{T-1} \langle \Delta_t, X_* - X_t \rangle + n\|C\|. \quad (5.7)$$

Now by Lemma 11,

$$\sum_{t=0}^{T-1} \|\tilde{G}_t\|^2 \leq c_{T,m,\delta}^2 c_h^2 T \quad (5.8)$$

with probability at least $1 - \delta/2$, so finally we turn toward the control of the random variable $\sum_{t=0}^{T-1} y_t$, where $y_t := \langle \Delta_t, X_* - X_t \rangle$.

Evidently $\{y_t\}_{t=0}^{T-1}$ is adapted to the filtration $\{\mathcal{F}_t\}_{t=0}^{T-1}$, and moreover, since X_t is measurable with respect to \mathcal{F}_{t-1} , we also have $\mathbb{E}[y_t | \mathcal{F}_{t-1}] = 0$. Therefore $\{y_t\}$ is a martingale difference sequence in the sense of Definition 9. Also, by Lemma 12, y_t is sub-exponential with parameters $(2\sqrt{n}c_h, 4c_h)$, conditioned on \mathcal{F}_{t-1} . (We are using the immediate fact that $\|X_t\|_F \leq \sqrt{n}$, since $X_t \in \mathcal{X}$.) Then by Theorem 10, we have that $\sum_{t=0}^{T-1} y_t$ is sub-exponential with parameters $(2\sqrt{Tn}c_h, 4c_h)$. We can always loosen these parameters a bit to say that $\sum_{t=0}^{T-1} y_t$ is sub-exponential with parameters $(2\sqrt{Tn}c_h, 4\sqrt{Tn}c_h)$ and then apply Corollary 7 to deduce that

$$\sum_{t=0}^{T-1} y_t \leq 2 \left(\frac{1}{2} + 4\log(2/\delta) \right) \sqrt{Tn}c_h \leq c_{T,m,\delta}c_h\sqrt{Tn} \quad (5.9)$$

with probability at least $1 - \delta/2$.

Combining (5.7), (5.8), and (5.9), as well as Lemma 3, which says that $d_0 \leq n \log 2$, we see that

$$\sum_{t=0}^{T-1} [F_\beta(X_t) - F_\beta(X_*)] \leq \frac{n \log 2}{\eta} + \frac{n}{4}\eta c_{T,m,\delta}^2 c_h^2 T + c_{T,m,\delta}c_h\sqrt{Tn} + n\|C\|$$

with probability at least $1 - \delta$. By taking $\eta = \frac{1}{c_{T,m,\delta}c_h\sqrt{T}}$, we complete the proof. \square

6 Structure of the energy

Now we elucidate the composition of the energy function $E(X)$ introduced above in Section 2 and explain how to understand the quantities $\|C - \mu\mathbf{I}\|$ and $c_h = c_\Psi\|V\|_\infty$ appearing in our convergence analysis in terms of the underlying physical problem. Our analysis does not rely on the presentation outlined in this section, which is included only for physical motivation and context. We include a discussion of general stochastic DFT beyond the Hartree approximation in Appendix D, where we also offer some commentary on the broader implications of our analysis.

6.1 Single-electron term

C is the matrix of the single-particle part of the quantum chemistry Hamiltonian in the $\{\psi_i\}$ basis:

$$C_{ij} = \int \psi_i(x) \left[-\frac{1}{2}\Delta + v_{\text{ext}} \right] \psi_j(x) dx,$$

where v_{ext} denotes the diagonal external potential. Typically the chemical potential should be chosen to lie within the spectrum of C . In this case $\|C - \mu\mathbf{I}\| \leq \|C\|$. It is common to assume some bound on $\|C\|$ for many calculations within a quantum chemistry basis. We defer discussion of the complete basis set limit (in which $\|C\|$ is unbounded) to Section 8.

6.2 Electron repulsion integrals

Recall from (2.3) that we assume the following structure for the ERI tensor

$$v_{ij,kl} = \sum_{p,q=1}^m \Psi_{pi} \Psi_{pj} V_{pq} \Psi_{qk} \Psi_{ql}, \quad (6.1)$$

where V is positive semidefinite and Ψ has orthonormal columns. This tensor should satisfy [33]

$$v_{ij,kl} \approx \int \psi_i(x) \psi_j(x) v_{\text{ee}}(x-y) \psi_k(y) \psi_l(y) dx dy, \quad (6.2)$$

where v_{ee} is the potential of the electron-electron interaction which defines a positive semidefinite kernel $v_{\text{ee}}(x-y)$. In electronic structure we typically have the Coulomb potential $v_{\text{ee}}(z) = \frac{1}{|z|}$, but it is also interesting to consider for example the case of the Yukawa potential $v_{\text{ee}}(z) = \frac{e^{-\alpha|z|}}{|z|}$ modeling screened interactions.

To understand how (6.1), which can be viewed as a tensor hypercontraction (THC) format [15, 32, 16] for the ERI, is related to (6.2), let $\{\phi_p\}_{p=1}^m$ denote a collection of interpolating functions associated to a collection interpolation points $\{x_p\}_{p=1}^m$ satisfying

$$w_p := \int \phi_p(x) dx > 0$$

and

$$g(x) \approx \sum_{p=1}^m g(x_p) \phi_p(x) \quad (6.3)$$

for functions g that are sufficiently smooth on a suitable region of support. Since quantum chemistry basis functions are typically smooth and effectively compactly supported (with exponentially decaying tails), it is reasonable to assume that m can be taken to be proportional to the volume of the computational domain, with $\{x_p\}_{p=1}^m$ taken to be equispaced grid points and $\{\phi_p\}_{p=1}^m$ chosen to be an interpolating Meyer wavelet basis [8] or a more compactly supported alternative such as a gausslet basis [39], while maintaining that (6.3) holds with high accuracy for all choices $g = \psi_i \psi_j$. (The accuracy can be reasonably assumed to be spectral with respect to m .)

In turn it follows that the approximation

$$\psi_i(x)\psi_j(x) \approx \sum_{p=1}^m \psi_i(x_p) \psi_j(x_p) \phi_p(x)$$

can be substituted into the right-hand side of (6.2) to justify the approximation, where we define V and Ψ in (2.3) by

$$V_{pq} = \frac{1}{w_p w_q} \int \phi_p(x) v_{ee}(x-y) \phi_q(y) dx dy$$

and

$$\Psi_{pi} \approx \tilde{\Psi}_{pi} := \psi_i(x_p) \sqrt{w_p}. \quad (6.4)$$

By construction V is positive semidefinite. Moreover

$$[\tilde{\Psi}^\top \tilde{\Psi}]_{ij} = \sum_p \psi_i(x_p) \psi_j(x_p) w_p = \int \sum_{p=1}^m \psi_i(x_p) \psi_j(x_p) \phi(x) dx \approx \int \psi_i(x) \psi_j(x) dx = \delta_{ij},$$

i.e., $\tilde{\Psi}$ almost has orthonormal columns. Therefore we can take Ψ to be approximately equal to $\tilde{\Psi}$ but satisfying $\Psi^\top \Psi = \mathbf{I}_n$ exactly, e.g., by symmetric orthogonalization $\Psi = \tilde{\Psi}(\tilde{\Psi}^\top \tilde{\Psi})^{-1/2}$.

In our analysis, we have taken the perspective that it is simpler to assume that the format (6.1) holds exactly for the ERI and perform analysis given this format, rather than work with the right-hand side of (6.2) directly. The preceding arguments justify that this format can be reasonably assumed, but a full analysis of the approximation is orthogonal to our efforts in this work, as the THC format is widely used in quantum chemistry calculations [15, 32, 16]. Moreover, the THC format is important from an implementation point of view in that it allows for the construction of the gradient estimator via the fast construction of the discrete electron density $\hat{\rho}_t$, following (4.1). Indeed, in more general stochastic DFT, it is important to lift the quantum chemistry basis representation to a grid-based representation in order to implement more general density functionals [12].

Now we want to explain how the quantity $c_h = c_\Psi \|V\|_\infty$ appearing in our analysis can be understood physically. For simplicity, assume (as is the case for our choices of interpolating basis described above) that $w_p = w$ is uniform, that $\frac{1}{w} \int |\phi_q(x)| dx = O(1)$, and that $\sum_{q=1}^m |\phi_q(x)| = O(1)$ in the thermodynamic limit. Also assume that all the basis functions $\{\psi_i\}$ are supported on some computational domain \mathcal{D} .

Then define the constants:

$$c_\psi := \sup_x \left\{ \sum_{i=1}^n |\psi_i(x)|^2 \right\}, \quad c_{ee} := \sup_{x \in \mathcal{D}} \int |v_{ee}(x-y)| dy.$$

Under the reasonable assumption that each of our quantum chemistry basis functions effectively overlaps with only $O(1)$ other basis functions in the thermodynamic limit, it is reasonable to assume that $c_\psi = O(1)$ in this limit. Moreover, if v_{ee} has rapid decay as in the case of the Yukawa potential, then $c_{ee} = O(1)$ as well.

Meanwhile, for Ψ as constructed in (6.4), $c_\Psi \lesssim w c_\psi$. Moreover, under our stated assumptions, $\sum_{q=1}^m |V_{pq}| = O(c_{ee}/w)$. Therefore $\|V\|_\infty = O(c_{ee}/w)$, and in turn

$$c_h = O(c_\psi c_{ee}).$$

Under the assumptions outlined above, this upper bound is $O(1)$ in the thermodynamic limit.

However, if v_{ee} is the Coulomb potential, c_{ee} will grow as the volume of the computational domain grows. This is a fair conclusion since the total Hartree energy grows proportionally as well, so the error bound that we achieve in Theorem 17 is still accurate in relative terms.

7 Chemical potential optimization

In this section we explain how an oracle for the unconstrained problem (2.1) can be used to solve the problem (2.2) in which the optimization variable X satisfies the particle number constraint $\text{Tr}[X] = N$, where $N \in [0, n]$. It is useful to define the **filling factor**

$$\nu = \frac{N}{n} \in (0, 1),$$

i.e., the number of electrons per basis function.

Let

$$g_\beta(\mu) := \sup_{0 \preceq X \preceq \mathbf{I}_n} \{\mu \text{Tr}[X] - F_\beta(X)\} \quad (7.1)$$

denote the negative of the optimal value of the unconstrained problem (2.1) as a function of the chemical potential μ .

Then the dual problem for the constrained problem (2.2) is precisely to maximize the concave objective

$$g_{N,\beta}(\mu) := N\mu - g_\beta(\mu) \quad (7.2)$$

over $\mu \in \mathbb{R}$.

We will use our oracle for approximately solving the unconstrained problem (2.1) as an approximate evaluator for this objective $g_{N,\beta}$. We want to show that it will suffice to apply this objective at a finite collection of values μ . For this to be the case, we want (1) to show that $g_{N,\beta}$ is Lipschitz and (2) to determine *a priori* bounds on the location of the maximizer. These tasks are accomplished via the following two lemmas, which are proved in Appendix E

Lemma 21. $g_{N,\beta} : \mathbb{R} \rightarrow \mathbb{R}$ is Lipschitz with Lipschitz constant n .

Lemma 22. The maximum of $g_{N,\beta}$ is attained within the interval

$$[\lambda_{\min}(C) - c_h - \beta^{-1} \log(\gamma^{-1}), \lambda_{\max}(C) + c_h + \beta^{-1} \log([1 - \gamma]^{-1})].$$

This holds even for $\beta = +\infty$, interpreting the terms involving β as zero.

Then for positive integer M , let μ_k , $k = 0, \dots, K$, denote equispaced points with

$$\mu_0 = \lambda_{\min}(C) - c_h - \beta^{-1} \log(\gamma^{-1}), \quad \mu_K = \lambda_{\max}(C) + c_h + \beta^{-1} \log([1 - \gamma]^{-1}).$$

We can solve (2.1) with $\mu = \mu_k$, for each $k = 0, \dots, K$ using algorithm (3.1), with step size chosen as in Theorem 17 for a given failure probability $\delta/(K+1)$, so that by the union bound we are guaranteed that the estimate of Theorem 17 succeeds for all k with probability at least $1 - \delta$. For each k , use the Cesàro mean \bar{X}_T over T iterations (cf. Theorem 17) to produce an estimate $\hat{g}_{N,\beta,k} \approx g_{N,\beta}(\mu_k)$. Then let $\hat{g}_{N,\beta} := \max_{k=0,\dots,K} \hat{g}_{N,\beta,k}$ denote the maximum estimated value.

Proposition 23. *Let p^* denote the optimal value of (2.2). The estimate $\hat{g}_{N,\beta}$ furnished by the above procedure satisfies*

$$\frac{|\hat{g}_{N,\beta} - p^*|}{n} = O\left(\frac{c_h \log(KTm/\delta)}{\sqrt{T}} + \left[\frac{1}{T} + \frac{1}{M}\right] \left[\|C\| + c_h + \beta^{-1} \log\left(\frac{1}{\gamma(1-\gamma)}\right)\right]\right)$$

holds with probability at least $1 - \delta$. Again the term involving β can be ignored if $\beta = +\infty$.

The proof is also given in Appendix E.

8 Complete basis set limit

In the complete basis set limit, where we consider an increasing number of basis functions per unit volume, there are two problems with the preceding analysis. First, the norm $\|C\|$ becomes unbounded due to the fact that the Galerkin projection of the Laplacian operator becomes unbounded in the complete basis set limit. Second, the size n of the basis set no longer remains within a fixed proportion of the number of electrons, and the free energy density per basis function F_β/n appearing in Theorem 17 is no longer physically meaningful.

Therefore in the complete basis set limit, we hope to provide an alternative to Theorem 17 which avoids any explicit dependence on $\|C\|$ or n . This will require some additional assumptions. Specifically, we must assume some sufficient growth in the eigenvalues of C , so that the high-energy eigenstates that arise from the finer discretization contribute only negligibly. We must also assume that the temperature is not arbitrarily high, so that entropic effects do not bestow nontrivial total occupation upon these high-energy eigenstates.

We note that to eliminate the dependence on $\|C\|$ and n from our analysis, we must pay the price of some dependence on β (which in particular we will assume to be finite). We will see that this dependence arises from the fact that we take an alternative initial condition X_0 , for which $D(X_\star \| X_0)$ depends on β .

Before formalizing the assumptions at which we have gestured above, we will phrase a convergence result more abstractly in terms of the quantities $D(X_\star \| X_0)$ and $\text{Tr}[X_0]$. We will also make the following simplifying assumption, which eases some of the notation in a few places.

Assumption 1. *In this section, assume that $\nabla \tilde{E}(X) \succeq 0$ for all $X \in \mathcal{X}$.*

Note that this assumption holds automatically for \tilde{E} induced by a choice of electron-electron potential $v_{ee} \geq 0$, such as the Yukawa or Coulomb potential. However, the assumption is not really necessary, and it can be guaranteed by replacing $C \leftarrow C - c_h \mathbf{I}_n$ while adopting the compensating change $\tilde{E}(X) \leftarrow \tilde{E}(X) + c_h \text{Tr}[X]$.

Moreover, note that Assumption 1 implies that our gradient estimator satisfies

$$\tilde{G}_t \succeq 0, \quad t = 0, \dots, T-1. \quad (8.1)$$

8.1 Initial condition and SCF interpretation

We do not change the mirror descent update rule (3.1), but we consider an alternative choice of initial condition, namely

$$X_0 = f_\beta(C - \mu \mathbf{I}_n),$$

which contrasts with our previous choice of $X_0 = f_\beta(0) = \mathbf{I}_n/2$. Equivalently, we start with effective Hamiltonian

$$H_0 = C - \mu \mathbf{I}_n.$$

It is instructive to recall (3.2), i.e., that the effective Hamiltonian update can be viewed as a convex combination:

$$H_{t+1} = (1 - \beta^{-1}\gamma_t)H_t + \beta^{-1}\gamma_t (G_t - \mu \mathbf{I}_n).$$

Therefore if we define the ‘effective potential’

$$V_t := H_t - (C - \mu \mathbf{I}_n),$$

we see that equivalently the effective potential satisfies the update rule

$$V_{t+1} = (1 - \beta^{-1}\gamma_t)V_t + (\beta^{-1}\gamma_t)\tilde{G}_t, \tag{8.2}$$

where we recall that \tilde{G}_t denotes our estimator for the Hartree potential $\nabla \tilde{E}(X_t)$. Since $H_0 = C - \mu \mathbf{I}_n$, the corresponding initial condition for this update is

$$V_0 = 0.$$

The effective Hamiltonian is recovered in terms of V_t via

$$H_t = C - \mu \mathbf{I}_n + V_t.$$

Therefore, the mirror descent update with this choice of initial condition coincides *precisely* with the ordinary self-consistent field (SCF) iteration [12] for the finite-temperature Hartree approximation with simple mixing, where the mixing parameter is $\beta^{-1}\gamma_t \in (0, 1)$, modulo the replacement of the Hartree potential with its stochastic estimator.

Note that the following lemma is immediate from (8.2), by the same logic as in the proof of Lemma 15:

Lemma 24. $0 \preceq V_t \preceq \tilde{g}_{\max} \mathbf{I}_n$ for all $t = 0, \dots, T-1$.

Proof. This follows via (8.2) from induction together with (8.1). \square

8.2 Key definitions and lemmas

Before proceeding with the convergence proof, we need a generalization of the strong convexity result (Lemma 2) which supplies a sharper strong convexity parameter for $S_{\text{FD}}(X)$ according to the trace of X (which shall remain bounded in the complete basis set limit for fixed volume).

Accordingly, we define

$$\mathcal{X}_\tau := \{X : 0 \preceq X \preceq \mathbf{I}_n, \quad \text{Tr}[X] \leq \tau\},$$

so $\mathcal{X}_\tau \subset \mathcal{X}_n = \mathcal{X}$. Then we prove:

Lemma 25. S_{FD} is $(1/\tau)$ -strongly convex on \mathcal{X}_τ with respect to the nuclear norm $\|\cdot\|_*$.

The proof is given in Appendix F.

In the complete basis set limit, we also cannot rely on $c_h = \|V\|_\infty c_\Psi$ (2.5) being bounded by a constant. The reason is that although it is possible to maintain that c_Ψ is bounded by a constant in the complete basis set limit, in fact $\|V\|_\infty$ scales with the density of basis functions per unit volume. (A concrete illustration will be offered in Section 9.3 below.) In fact, the main importance of c_h in our arguments above is in bounding terms related to the Hartree potential $\nabla \tilde{E}(X)$. In our preceding analysis, we use the trivial bound $\rho(X) \leq 1$ to bound the potential in terms of c_h . However, in the complete basis set limit (with a fixed number of electrons per unit volume), we expect that the occupation of any individual site will scale inversely with the density of basis functions per unit volume, so that the growth of $\|V\|_\infty$ and the decay of $\rho(X)$ compensate for each other.

Therefore it is more natural to rely on the quantity

$$\tilde{c}_h := \max \left(\| |V| \rho(X_\star) \|_\infty, \max_{t=0, \dots, T-1} \| |V| \rho(X_t) \|_\infty \right). \quad (8.3)$$

Here $|V|$ denotes the entrywise absolute value of V . For a non-negative electron-electron interaction $v_{ee} \geq 0$ and an interpolating basis as we shall consider in Section 9.3, naturally we will have $|V| = V$. Therefore following the interpretation of Section 6.2, \tilde{c}_h can be viewed as a bound on L^∞ norm of the spatial Hartree potential (evaluated on a set of interpolating points) over the optimization trajectory.

We will not provide any *a priori* bounds for this quantity, which would rely on more detailed analysis involving the composition of the single-particle matrix C as a sum of kinetic and potential terms (cf. Section 9.3). If the external potential v_{ext} is assumed to be bounded (as could be guaranteed via the use of a nuclear pseudopotential [13]), then since the Hartree potential is also uniformly bounded (via Lemma 24) over the optimization trajectory, the effective Hamiltonian H_t would consist of a kinetic (Laplacian term) together with a bounded effective potential. We conjecture that for reasonable choices of basis (such as the periodic sinc basis considered in Section 9 below), such assumptions would suffice for a suitable *a priori* bound for $\rho(X_t)$ over the optimization trajectory. However, such an analysis will take us outside the intended scope of our results, which we intend to phrase more naturally in terms of physical quantities and with a minimum of detailed assumptions. In any case, with or without *a priori* bounds, the quantity (8.3) is the physically relevant quantity to be featured in the analysis.

Before proceeding with the convergence proof, we need to rephrase some of our earlier lemmas more delicately in terms of \tilde{c}_h .

First, we modify Lemma 11 as follows:

Lemma 26. *For any $\delta \in (0, 1]$, the inequality*

$$\max_{t=0, \dots, T-1} \|\hat{G}_t\| \leq 2(1 + 4 \log(Tm/\delta)) \tilde{c}_h$$

holds with probability at least $1 - \delta$.

Second, we modify Lemma 12. We make the statement more specific, tailored precisely to how we will use the lemma (analogously to the use of Lemma 12 in the proof of Theorem 17).

Lemma 27. *For all $t = 0, \dots, T-1$, the random variable $\langle \Delta_t, X_\star - X_t \rangle$ is sub-exponential with parameters $(4\tilde{c}_h \|X_t\|_F, 8\tilde{c}_h)$, conditioned on \mathcal{F}_{t-1} .*

The proofs of both lemmas are in Appendix F.

8.3 Convergence theorem and proof

Theorem 28. For any $\delta \in (0, 1]$, define $c_{T,m,\delta} := 2(1 + 4\log(2Tm/\delta))$. Also let $\tau := \max(\text{Tr}[X_0], 1)$, where $X_0 = f_\beta(C - \mu \mathbf{I}_n)$ is the initial condition. Consider algorithm defined by (3.4) with step size $\eta_t = \eta := \sqrt{\frac{2D(X_\star \| X_0)}{\tau c_{T,m,\delta}^2 \tilde{c}_h^2 T}}$, or equivalently by (3.1) with $\gamma_t := \frac{\eta\beta}{\eta+\beta}$. Then

$$\frac{1}{T} \sum_{t=0}^{T-1} (F_\beta(X_t) - \mu \text{Tr}[X_t]) \leq F_\beta(X_\star) - \mu \text{Tr}[X_\star] + \frac{(\sqrt{2\tau D(X_\star \| X_0)} + 2\tau) c_{T,m,\delta} \tilde{c}_h}{\sqrt{T}}$$

holds with probability at least $1 - \delta$.

Proof. As in the proof of Theorem 17, we can assume without loss of generality that $\mu = 0$.

First we claim that

$$\text{Tr}[X_t] \leq \text{Tr}[X_0]$$

for all t .

To see this, recall that $X_t = f_\beta(H_t)$, and moreover $H_t = H_0 + V_t \succeq H_0$ by Lemma 24. Then Weyl's monotonicity theorem guarantees that

$$\lambda_k(H_t) \geq \lambda_k(H_0)$$

for all k , where λ_k denotes the k -th eigenvalue, ordered non-decreasingly. Then since f_β is a decreasing function, it follows that

$$\text{Tr}[X_t] = \sum_{k=1}^n f_\beta(\lambda_k(H_t)) \leq \sum_{k=1}^n f_\beta(\lambda_k(H_0)) = \text{Tr}[X_0],$$

as claimed. Since $\tau = \max(\text{Tr}[X_0], 1)$ it follows that $X_t \in \mathcal{X}_\tau$ for all t .

Again for simplicity, we replace $C \leftarrow C - \mu \mathbf{I}_n$ to ease the notation in the proof. Then by the exact same argument as in the proof of Theorem 17, where instead by way of Lemma 25 we use τ^{-1} in the place of $2/n$ as the strong convexity parameter, we deduce (cf. (5.6)) that

$$\begin{aligned} \sum_{t=0}^{T-1} [F_\beta(X_t) - F_\beta(X_\star)] &\leq \frac{1}{\eta} [d_0 - d_T] + \frac{\tau}{2} \eta \sum_{t=0}^{T-1} \|\tilde{G}_t\|^2 + \sum_{t=0}^{T-1} \langle \Delta_t, X_\star - X_t \rangle \\ &\quad + \langle C, X_0 - X_T \rangle + \frac{1}{\beta} [S_{\text{FD}}(X_0) - S_{\text{FD}}(X_T)]. \end{aligned}$$

Importantly, we can now group the last two terms in a meaningful way due to our choice of initial condition. Indeed, since $C = \frac{1}{\beta} \nabla S_{\text{FD}}(X_0)$, we can compute:

$$\begin{aligned} &\langle C, X_0 - X_T \rangle + \frac{1}{\beta} [S_{\text{FD}}(X_0) - S_{\text{FD}}(X_T)] \\ &= -\frac{1}{\beta} D(X_T \| X_0), \end{aligned}$$

which is in particular ≤ 0 .

Again, $d_T \geq 0$, so we deduce

$$\sum_{t=0}^{T-1} [F_\beta(X_t) - F_\beta(X_\star)] \leq \frac{d_0}{\eta} + \frac{\tau}{2} \eta \sum_{t=0}^{T-1} \|\tilde{G}_t\|^2 + \sum_{t=0}^{T-1} \langle \Delta_t, X_\star - X_t \rangle.$$

The bounding of the last two terms proceeds similarly to the proof of Theorem 17, except that we do not use the trivial bound $\|X_t\|_F \leq \sqrt{n}$ to control the sub-exponentiality parameters of $\sum_{t=0}^{T-1} \langle \Delta_t, X_\star - X_t \rangle$.

Indeed, carrying forward the argument without inserting this bound, we deduce from Lemma 27 and Theorem 10 that $\sum_{t=0}^{T-1} \langle \Delta_t, X_\star - X_t \rangle$ is sub-exponential with parameters $(4\sqrt{T}\|X_t\|_F \tilde{c}_h, 8\tilde{c}_h)$. Now $\|X_t\|_F \leq \text{Tr}[X_t]$ since $X_t \succeq 0$, and in turn $\text{Tr}[X_t] \leq \tau$. Therefore, since $\tau \geq 1$, we can loosen the sub-exponentiality parameters to $(4\tau\sqrt{T}\tilde{c}_h, 8\tau\sqrt{T}\tilde{c}_h)$ and apply Corollary 7 to deduce that

$$\sum_{t=0}^{T-1} \langle \Delta_t, X_\star - X_t \rangle \leq 2\tau c_{T,m,\delta} \tilde{c}_h \sqrt{T}$$

with probability at least $1 - \delta/2$. (Compare with (5.9). Relative to that inequality, we have simply replaced \sqrt{n} in the right-hand side with τ and c_h with \tilde{c}_h .)

Similarly to the proof of Theorem 10 (except that we use Lemma 26 in the place of Lemma 11), we can bound

$$\sum_{t=0}^{T-1} \|\tilde{G}_t\|^2 \leq c_{T,m,\delta}^2 \tilde{c}_h^2 T$$

with probability at least $1 - \delta/2$.

Then it follows that

$$\sum_{t=0}^{T-1} [F_\beta(X_t) - F_\beta(X_\star)] \leq \frac{d_0}{\eta} + \frac{\tau}{2} \eta c_{T,m,\delta}^2 \tilde{c}_h^2 T + 2\tau c_{T,m,\delta} \tilde{c}_h \sqrt{T}$$

holds with probability at least $1 - \delta$.

By choosing

$$\eta = \sqrt{\frac{d_0}{\frac{\tau}{2} c_{T,m,\delta}^2 \tilde{c}_h^2 T}},$$

we complete the proof. \square

8.4 Control in terms of eigenvalue growth

Note that in Theorem 28, the explicit dependence on $\|C\|$ and n have been eliminated. However, we want to argue that $\text{Tr}[X_0]$ and $D(X_\star\|X_0)$ remain bounded independent of these quantities in the complete basis set limit.

In order to control these quantities, we must assume some model of eigenvalue growth for the single-particle Hamiltonian matrix C . Throughout we let $\lambda_k(A)$, $k = 1, \dots, n$, denote the k -th eigenvalue of a symmetric matrix A , counted in non-decreasing order. Then the eigenvalue growth assumption is as follows.

Assumption 2. Assume that $\lambda_k(C) \geq (k/c_\lambda)^\alpha$ for some constant $\alpha, c_\lambda > 0$.

Note that this assumption is naturally satisfied (after a suitable scalar shift) with $\alpha = 2/d_{\text{eff}}$ for quasi- d_{eff} -dimensional systems due to the growth of the eigenvalues of the Laplacian, in both the thermodynamic and complete basis set limits. Intuitively, we can think of c_λ as proportional to the d_{eff} -dimensional volume or the number of atoms in the problem. We will not pursue a detailed analysis guaranteeing the assumption since it is orthogonal to the content of this work.

It is somewhat cumbersome to deal with the case of general α , so for simplicity we simply take $\alpha = 1$ in the ensuing analysis. The numerical constants that we obtain are not so physically relevant anyway—the asymptotic eigenvalue growth kicks in once we have entered the scattering part of the spectrum, while in practice we are mostly interested in a chemical potential that targets the bound states. Our main goal is simply to demonstrate the dependence of the quantities $\text{Tr}[X_0]$ and $D(X_\star \| X_0)$ on β , c_h , and c_λ , as well as to verify their independence from $\|C\|$ and n . The dependence on μ that we obtain is less physically relevant. For these reasons, we are content to adopt the simplifying assumption $\alpha = 1$. The heuristic conclusions do not change in the general case.

Now we state two lemmas bounding $\text{Tr}[X_0]$ and $D(X_\star \| X_0)$, respectively. The proofs are given in Appendix F.

Lemma 29. Suppose that Assumption 2 holds with $\alpha = 1$. Then

$$\text{Tr}[X_0] \leq c_\lambda(\mu + \beta^{-1}) + 1.$$

Suppose that Assumption 2 holds with $\alpha = 1$. Then

$$D(X_\star \| X_0) \leq c_\lambda [(2\beta c_h + 1)\mu + 4\beta^{-1}] + 2.$$

These two lemmas, together with Theorem 28, immediately imply the following.

Corollary 30. Suppose that Assumption 2 holds with $\alpha = 1$. Also suppose $\beta \geq 1$. Under the same hypotheses as in the statement of Theorem 28, the inequality

$$\frac{1}{T} \sum_{t=0}^{T-1} (F_\beta(X_t) - \mu \text{Tr}[X_t]) \leq F_\beta(X_\star) - \mu \text{Tr}[X_\star] + O\left(\frac{\log(Tm/\delta) (1 + \sqrt{\beta c_h}) \tilde{c}_h n_{\text{eff}}}{\sqrt{T}}\right)$$

holds with probability at least $1 - \delta$, where $n_{\text{eff}} := 1 + c_\lambda[\mu + \beta^{-1}]$.

Remark 31. Following Assumption 2, it is reasonable to think of n_{eff} as something akin to an effective basis set size which remains in proportion with the particle number. Importantly, it remains proportional to the volume (i.e., proportional to c_λ) in the thermodynamic and complete basis set limits (even taken simultaneously).

9 Numerical experiments

Now we describe several numerical experiments supporting our theory.

We will consider functions on the box domain $\mathcal{D} := \prod_{j=1}^d [0, L_j]^d$ where d is the spatial dimension and L_1, \dots, L_d are the box dimensions, with periodic boundary conditions. We will consider a

Galerkin discretization in the periodic sinc (or planewave dual) basis [4] for this periodic domain. This basis is equivalent in its span to a suitable planewave basis, but the interpolating property of the periodic sinc basis will allow us to represent diagonal potentials more conveniently via a pseudospectral approximation [4].

9.1 Domain and basis

Adopt the notation $[j] := \{0, \dots, j-1\}$ for arbitrary non-negative integer j .

Now let n_i denote the number of grid points / basis functions in dimension $i = 1, \dots, d$. Accordingly let $\mathcal{I} := \prod_{i=1}^d [n_i]$ denote the indexing set for our computational grid, and define grid points

$$\mathbf{x}_{\mathbf{j}} := \mathbf{j}\Delta\mathbf{x} = (j_1\Delta x_1, \dots, j_d\Delta x_d)$$

indexed by $\mathbf{j} \in \mathcal{I}$. Here $\Delta x_i = \frac{L_i}{n_i}$ is the mesh size in each dimension, $\Delta\mathbf{x} = (\Delta x_1, \dots, \Delta x_d)$, and n_i is an *odd* integer number of discretization points per dimension.

It is also useful to define $\mathcal{V} := \prod_{i=1}^d L_i$ (the domain volume), $n = \prod_{i=1}^d n_i$ (the total number of grid points / basis functions), $\mathbf{n} = (n_1, \dots, n_d)$, and $\Delta\mathcal{V} = \mathcal{V}/n$ (the discrete volume element).

Next, we define the planewaves adapted to this periodic box by

$$e_{\mathbf{k}}(\mathbf{x}) := \frac{1}{\sqrt{\mathcal{V}}} e^{2\pi i \mathbf{k} \cdot (\mathbf{x}/\mathbf{L})}, \quad \mathbf{k} \in \hat{\mathcal{I}},$$

where our dual indexing set $\hat{\mathcal{I}}$ is defined by

$$\hat{\mathcal{I}} := \prod_{i=1}^d \{-\ell_i, \dots, \ell_i\}, \quad \ell_i := (n_i - 1)/2$$

and vector quotients are interpreted elementwise. The set $\{e_{\mathbf{k}}\}_{\mathbf{k} \in \hat{\mathcal{I}}}$ is orthonormal with respect to the $L^2(\mathcal{D})$ inner product, which we denote by $\langle \cdot, \cdot \rangle$.

Then the periodic sinc basis $\{\psi_{\mathbf{j}}\}_{\mathbf{j} \in \mathcal{I}}$ is defined by periodic translation of a reference basis function:

$$\psi_{\mathbf{j}}(\mathbf{x}) = \psi_{\mathbf{0}}(\mathbf{x} - \mathbf{j}\Delta\mathbf{x}),$$

where the reference is in turn defined as

$$\psi_{\mathbf{0}}(\mathbf{x}) := \frac{1}{\sqrt{\Delta\mathcal{V}}} \prod_{i=1}^d \frac{\sin(\pi m_i x_i / L_i)}{m_i \sin(\pi x_i / L_i)}$$

and vector products are interpreted elementwise.

The set $\{\psi_{\mathbf{j}}\}_{\mathbf{j} \in \mathcal{I}}$ is also orthonormal with respect to the $L^2(\mathcal{D})$ inner product. Moreover, these functions can be written in terms of planewaves via the unitary transformation:

$$\psi_{\mathbf{j}} = \frac{1}{\sqrt{n}} \sum_{\mathbf{k} \in \hat{\mathcal{I}}} e^{-2\pi i \mathbf{k} \cdot (\mathbf{j}/\mathbf{n})} e_{\mathbf{k}}.$$

Finally, $\{\psi_{\mathbf{j}}\}$ can be rescaled to obtain a basis

$$\phi_{\mathbf{j}} := \psi_{\mathbf{j}} \sqrt{\Delta\mathcal{V}},$$

which is an interpolating basis for the grid $\{x_j\}$ in the sense that

$$f(x) = \sum_{\mathbf{j} \in \mathcal{I}} f(\mathbf{x}_j) \phi_j(x)$$

for f lying in the span of trigonometric polynomials (suitably scaled to our periodic domain) of multivariate order up to $(\frac{n_1-1}{2}, \dots, \frac{n_d-1}{2})$. In particular, our periodic sinc basis includes all such planewaves in its complex span.

9.2 Single-particle matrix

The single-particle matrix (cf. Section 6.1)

$$C = K + U$$

is constructed from the discretizations of two terms: (1) the kinetic term and (2) the diagonal external potential v_{ext} .

The kinetic matrix K is produced by direct Galerkin projection. We have

$$K_{\mathbf{j}, \mathbf{j}'} = -\frac{1}{2} \int_{\mathcal{D}} \psi_j(x) \Delta \psi_{j'}(x) dx.$$

Now the Laplacian is translation-invariant, so $K_{\mathbf{j}, \mathbf{j}'} = K_{\mathbf{j}-\mathbf{j}', 0}$ is determined by a single row (or column) and can be diagonalized by the d -dimensional unitary discrete Fourier transform \mathcal{F} (with dual indexing set $\hat{\mathcal{I}}$). One can compute:

$$K = \frac{1}{2} \mathcal{F} D \mathcal{F}^*$$

where $D = \text{diag}(d)$ is a diagonal matrix, defined by

$$d_{\mathbf{k}} = \sum_{i=1}^d (2\pi k_i / L_i)^2, \quad \mathbf{k} \in \hat{\mathcal{I}}.$$

Meanwhile, the external potential is discretized within the pseudospectral approximation [4] via $U = \text{diag}(u)$ where

$$u_j = v_{\text{ext}}(\mathbf{x}_j), \quad \mathbf{j} \in \mathcal{I}.$$

9.3 Hartree contribution

It remains to describe how the ERI (2.3) are constructed. In our case, the ‘interpolating basis’ size m (cf. Section 6.2) coincides with the basis set size n .

We follow the construction and notation outlined in Section 6.2, only changing the indexing notation to coincide with our multi-indexing convention. Then to specify the ERI (2.3), we need to fix $\Psi_{\mathbf{p}\mathbf{j}}$ (an $n \times n$ unitary matrix) as well as $V_{\mathbf{p}\mathbf{q}}$ (an $n \times n$ positive semidefinite matrix).

It is elementary to verify that the interpolating basis weights $w_{\mathbf{p}} = \int_{\mathcal{D}} \phi_{\mathbf{p}}(x) dx$ are all given by $w_{\mathbf{p}} = \Delta \mathcal{V}$. Moreover,

$$\Psi_{\mathbf{p}\mathbf{j}} := \psi_j(x_{\mathbf{p}}) \sqrt{w_{\mathbf{p}}} = \delta_{\mathbf{p}\mathbf{j}}$$

is the identity (hence in particular unitary without need for correction), and finally, still following Section 6.2, we take

$$V_{\mathbf{p}\mathbf{q}} = \frac{1}{\Delta\mathcal{V}} \int_{\mathcal{D}} \psi_{\mathbf{p}}(x) v_{\text{ee}}(x-y) \psi_{\mathbf{q}}(y) dx dy.$$

Now V , like K , is diagonalized by the unitary discrete Fourier transform, and we can write

$$V = \frac{1}{\Delta\mathcal{V}} \mathcal{F} \hat{V} \mathcal{F}^*,$$

where $\hat{V} = \text{diag}(\hat{v})$.

To implement the Yukawa interaction, we define \hat{v} as

$$\hat{v}_{\mathbf{k}} = \frac{\alpha^2}{\alpha^2 + \sum_{i=1}^d (2\pi k_i / L_i)^2}$$

The Coulomb interaction can be recovered by setting $\alpha = 0$ and setting $\hat{v}_0 = 0$. (Note that more generally, the $\mathbf{k} = 0$ mode can be removed, since this will simply contribute a constant shift to the Hartree potential.)

Importantly, note that for this choice of basis many of the general constructions outlined above simplify intuitively. First, we have simply

$$\rho(X) = \text{diag}(X),$$

and in turn

$$\tilde{E}(X) = \frac{1}{2} \rho(X)^\top V \rho(X), \quad \nabla \tilde{E}(X) = \text{diag}^* [V \rho(X)].$$

Meanwhile, the gradient estimator can be constructed by first defining

$$\hat{\rho}_t = (X_t^{1/2} z_t)^{\odot 2}$$

and then

$$\tilde{G}_t = \text{diag}^* [V \hat{\rho}_t].$$

The computational difficulties lie in (1) the matrix-vector multiplication $X_t^{1/2} z_t$, which we implement via the contour method (cf. Appendix C) that is robust to both the thermodynamic and complete basis set limits and (2) the matrix-vector multiplication $V \hat{\rho}_t$, which we implement via FFTs. (Note that to implement the contour approach, we must in particular call fast matrix-vector multiplications by H_t , which can themselves be reduced to diagonal matrix operations via FFTs.)

9.4 Numerical results

We conduct experiments running the mirror descent (3.2) for the periodic discretization outlined above. In particular, we examine the algorithm's robustness by varying the box size, grid resolution, inverse temperature, and spatial dimension. All of our numerical experiments are implemented in JAX, and the code is publicly available at

<https://github.com/willcai7/MirrorDescent-DFT>

Hardware. Each experiment was carried out using a single Nvidia A100 GPU, equipped with 80GB of memory.

Problem specification. Our objective function consists of several terms. We set the Yukawa parameter to $\alpha = 0.5$ to define the Hartree contribution. To generate the external potential, we first create a random background charge distribution by uniformly sampling $\lfloor \zeta V \rfloor$ points from our grid and assigning them each an equal unit ‘charge.’ The external potential is then given by $v_{\text{ext}} = -V\rho_{\text{ext}}$, where V is the discretized Yukawa kernel defined above with $\alpha = 0.5$. In our simulations, we fix $\zeta = 1$ and set the chemical potential to $\mu = 0$. We always choose a cubic domain, i.e., $\mathbf{L} = L\mathbf{1}_d$ for varying L .

Mirror descent. Our simulations adopt an exponential decay schedule for the step size, given by

$$\gamma_t = \gamma \cdot \exp(-t/1000).$$

For most simulations, we use a step-size of $\gamma = 1$; however, when $\beta = 0.5$, we reduce the step-size to $\gamma = 0.5$. The reason for deviating from the theoretical prescription for the step size is that in the theory it is more convenient to consider a finite time horizon that is specified *a priori*. But in practice, it is easier to manage an infinite time horizon with a decay schedule. We chose the exponential schedule for its robust practical performance. Similar considerations often apply in analysis of other mirror descent algorithms. We run the mirror descent for a maximum of 5000 iterations, and we initialize with $H_0 = C - \mu I$.

Contour method. To estimate the gradient for the Hartree contribution in the objective, we employ the contour method outlined in Appendix C. We refer to a single approximate matrix-vector multiplication by $f_\beta^{1/2}(H_t)$ as a ‘contour matvec.’ We set the number of poles to 20. Within this method, we use the BiCGSTAB linear solver [35] with a maximum of 1000 iterations and a tolerance of 10^{-5} to solve the linear systems. The preconditioner is chosen as in Appendix C.2. Unlike our theoretical analysis, which uses a single Gaussian sample to define the gradient estimator in each iteration, our experiments perform an empirical average over N_g Gaussian samples. This allows us to exploit GPU parallelism for the implementation of a batch of N_g contour matvecs. We typically use $N_g = 20$, except for our largest experiments where we use $N_g = 10$ (cf. Table 1). We denote the batch of Gaussian samples at each iteration as $z_t \in \mathbb{R}^{n \times N_g}$, where each column of z_t represents a single Gaussian sample.

Evaluation. We assess convergence by comparing our results against the final output of the deterministic SCF algorithm (for problems that are small enough such that it is tractable) which serves as our ground truth. When the exact ground truth is available, we report the relative errors of the density function along with the absolute errors in the free energy density, Hartree energy density, and number of electrons per volume. Additionally, we define a “**gold standard**” method as a benchmark for evaluating the convergence of the density functions. The gold standard assumes access to the exact optimizer X_\star and then estimates the density using the same Gaussian samples z_t , i.e., it completely avoids the optimization. As such it is not supposed to define a realistic scalable algorithm. Rather, we wish to demonstrate that our scalable algorithm performs similarly to this unrealistic gold standard. Specifically, the gold standard defines the density by

$$\hat{\rho}_{\text{gold},t} = \frac{\text{diag}[\sum_{i=1}^t (X_\star^{1/2} z_t) \cdot (X_\star^{1/2} z_t)^\top]}{N_g \cdot t}.$$

Numerical results. Figures 9.1, 9.2, 9.3, 9.4, 9.5, and 9.6 display the external potentials, final density functions, relative density errors, Hartree energy densities, free energy densities, and

electrons per volume across various dimensions, inverse temperatures, grid resolutions, and box sizes. In all plots, at each iteration we average the results from the latter half of the mirror descent iterations completed thus far, in order to define asymptotically consistent estimators. Several key observations emerge:

- **Robustness in two limits.** The mirror descent algorithm shows strong performance in both the thermodynamic and complete basis set limits. In Figures 9.1, 9.3, and 9.5, subplots (a) and (b) highlight its robustness in the thermodynamic limit, while subplots (b) and (c) confirm its stability in the complete basis limit.
- **Robustness with respect to inverse temperatures and dimensions.** Figures 9.2, 9.4, and 9.6 support the algorithm’s resilience against variations in inverse temperature, and all figures collectively demonstrate consistent performance across different dimensions.
- **Comparable performance to the “gold standard” method.** Across all settings, mirror descent performs nearly on par with the “gold standard” method, implying that its computational complexity is almost equivalent to that of estimating the density given the converged optimizer.

Furthermore, we applied mirror descent to two large 3D systems, as shown in Figure 9.7. For a grid size of $\mathbf{n} = (101, 101, 101)$, the density matrix exceeds $10^6 \times 10^6$ in size. While deterministic SCF becomes intractable at this scale, our stochastic mirror descent approach converges as efficiently as it does for smaller systems. This result highlights the capability of stochastic mirror descent to handle much larger systems than SCF.

Wall clock. Table 1 provides a comprehensive summary of the scaling of the average wall clock time T_{vec} of a batch of N_g contour matvecs. The averages are computed by taking an empirical average over the optimization trajectory with a stride length of 20 iterations. We also report T_{vec}/n for all simulations. (We report the time for a batch of contour matvecs rather than individual ones, since the batched BiCGSTAB solver in JAX exhibits nonlinear scaling with respect to the number N_g of Gaussian samples, due to parallelism.) Several key observations can be made from these results:

- **Scaling with inverse temperature:** The data for the simulations in Figures 9.2, 9.4, and 9.6 suggest that the average contour matvec time scales as $O(\sqrt{\beta})$ with respect to the inverse temperature β . Although we cannot prove this aspect of the scaling theoretically for the contour method, it matches the scaling conjectured in the introduction.
- **Complete basis set limit:** The data for the simulations in the (a) and (b) subplots of Figures 9.1, 9.3, and 9.5 reveal that the average contour matvec time scales close to $O(n)$ with respect to the number n of grid points as the grid spacing is refined for a fixed volume. This validates our notion of optimal scaling in the complete basis set limit.
- **Scaling with box size:** The data for simulations in the (b) and (c) subplots of Figures 9.1, 9.3, and 9.5, along with those in (a) and (b) of Figure 9.7, demonstrate that the average contour matvec time is largely insensitive to increases in the box size.

Overall, these numerical results underscore the efficiency, robustness, and scalability of the mirror descent algorithm. The favorable scaling with respect to inverse temperature, grid resolution, and

Figure	n	L	β	γ	N_g	T_{vec} (s)	T_{vec}/n (s)
9.1.(a)	6	10	10	1.0	20	0.0139	2.32×10^{-3}
9.1.(b)	1281	10	10	1.0	20	0.0229	1.79×10^{-5}
9.1.(c)	12801	100	10	1.0	20	0.4565	3.57×10^{-5}
9.2.(a)	12801	100	0.5	0.5	20	0.0961	7.51×10^{-6}
9.2.(b)	12801	100	2	1.0	20	0.1971	1.54×10^{-5}
9.2.(c)	12801	100	40	1.0	20	0.7206	5.63×10^{-5}
9.3.(a)	(51,51)	(10,10)	10	1.0	20	0.0255	9.80×10^{-5}
9.3.(b)	(101,101)	(10,10)	10	1.0	20	0.0807	7.91×10^{-5}
9.3.(c)	(101,101)	(100,100)	10	1.0	20	0.1844	1.81×10^{-5}
9.4.(a)	(101,101)	(100,100)	0.5	0.5	20	0.0614	6.02×10^{-6}
9.4.(b)	(101,101)	(100,100)	2	1.0	20	0.0946	9.27×10^{-6}
9.4.(c)	(101,101)	(100,100)	40	1.0	20	0.5438	5.33×10^{-5}
9.5.(a)	(11,11,11)	(10,10,10)	10	1.0	20	0.0189	1.42×10^{-5}
9.5.(b)	(21,21,21)	(10,10,10)	10	1.0	20	0.0471	5.08×10^{-6}
9.5.(c)	(21,21,21)	(30,30,30)	10	1.0	20	0.0598	6.46×10^{-6}
9.6.(a)	(21,21,21)	(30,30,30)	0.5	0.5	20	0.0341	3.68×10^{-6}
9.6.(b)	(21,21,21)	(30,30,30)	2	1.0	20	0.0418	4.51×10^{-6}
9.6.(c)	(21,21,21)	(30,30,30)	40	1.0	20	0.0929	1.00×10^{-5}
9.7.(a)	(101,101,101)	(10,10,10)	10	1.0	10	3.4839	3.38×10^{-6}
9.7.(b)	(101,101,101)	(100,100,100)	10	1.0	10	5.2709	5.12×10^{-6}

Table 1: This table shows the average time T_{vec} of a batch of N_g contour matvecs, as well as T_{vec}/n , for all simulations. During each simulation, timings were recorded every 20 iterations and then aggregated to compute averages.

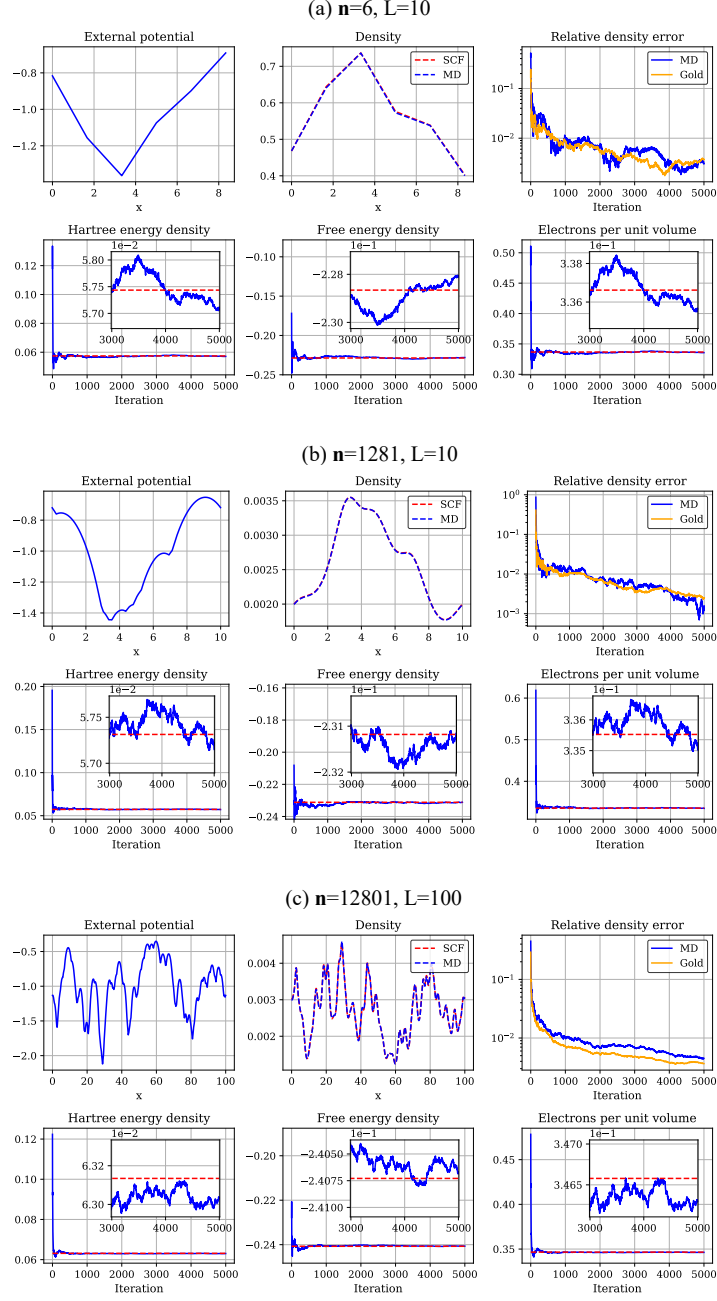


Figure 9.1: 1D simulation results of the mirror descent algorithm. Here we fix $\beta = 10$ and change the box size L and the grid size n . The blue and gold lines denote the results of the mirror descent and the gold standard, while the red dashed lines denote the final outputs of the deterministic SCF.

box size not only highlight the method’s computational efficiency but also its potential for application in large-scale simulations where time complexity is a critical factor.

References

- [1] Roi Baer, Daniel Neuhauser, and Eran Rabani. Self-averaging stochastic kohn-sham density-functional theory. *Phys. Rev. Lett.*, 111:106402, Sep 2013.
- [2] Amir Beck and Marc Teboulle. Mirror descent and nonlinear projected subgradient methods for convex optimization. *Operations Research Letters*, 31(3):167–175, 2003.
- [3] Amir Beck and Marc Teboulle. A fast iterative shrinkage-thresholding algorithm for linear inverse problems. *SIAM journal on imaging sciences*, 2(1):183–202, 2009.
- [4] John P. Boyd. *Chebyshev and Fourier spectral methods*. Dover Publications, Mineola, N.Y, 2nd ed., rev edition, 2001.
- [5] Eric A. Carlen and Elliott H. Lieb. Remainder terms for some quantum entropy inequalities. *Journal of Mathematical Physics*, 55(4):042201, 04 2014.
- [6] Gong Chen and Marc Teboulle. Convergence analysis of a proximal-like minimization algorithm using bregman functions. *SIAM Journal on Optimization*, 3(3):538–543, 1993.
- [7] Yael Cytter, Eran Rabani, Daniel Neuhauser, and Roi Baer. Stochastic Density Functional Theory at Finite Temperatures. *Physical Review B*, 97(11):115207, March 2018.
- [8] Ingrid Daubechies. *Ten Lectures on Wavelets*. Society for Industrial and Applied Mathematics, January 1992.
- [9] David A. Drabold and Otto F. Sankey. Maximum entropy approach for linear scaling in the electronic structure problem. *Phys. Rev. Lett.*, 70:3631–3634, Jun 1993.
- [10] Bradley Efron. *The Jackknife, the Bootstrap and Other Resampling Plans*. Society for Industrial and Applied Mathematics, January 1982.
- [11] Khaled Eldowa and Andrea Paudice. General Tail Bounds for Non-Smooth Stochastic Mirror Descent. In *Proceedings of The 27th International Conference on Artificial Intelligence and Statistics*, pages 3205–3213. PMLR, April 2024.
- [12] Marcel David Fabian, Ben Shpiro, Eran Rabani, Daniel Neuhauser, and Roi Baer. Stochastic density functional theory. *WIREs Computational Molecular Science*, 9(6), November 2019.
- [13] François Gygi. All-electron plane-wave electronic structure calculations. *Journal of Chemical Theory and Computation*, 19(4):1300–1309, 02 2023.
- [14] Nicholas Hale, Nicholas J Higham, and Lloyd N Trefethen. Computing a^α , $\log(a)$, and related matrix functions by contour integrals. *SIAM Journal on Numerical Analysis*, 46(5):2505–2523, 2008.

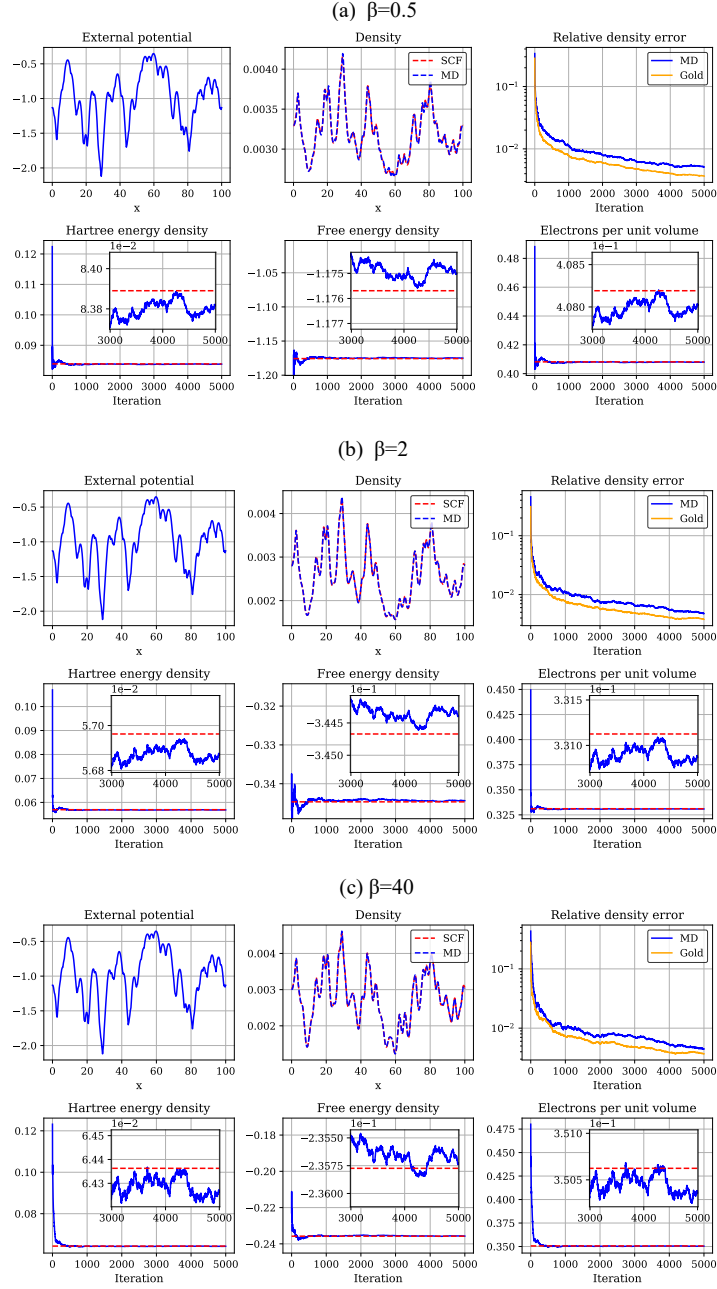


Figure 9.2: 1D simulation results of the mirror descent algorithm. We fix the grid size to be $n = 12801$ and the box size to be $L = 100$. We consider $\beta = 0.5, 2, 40$. The other settings are the same as in Figure 9.1.

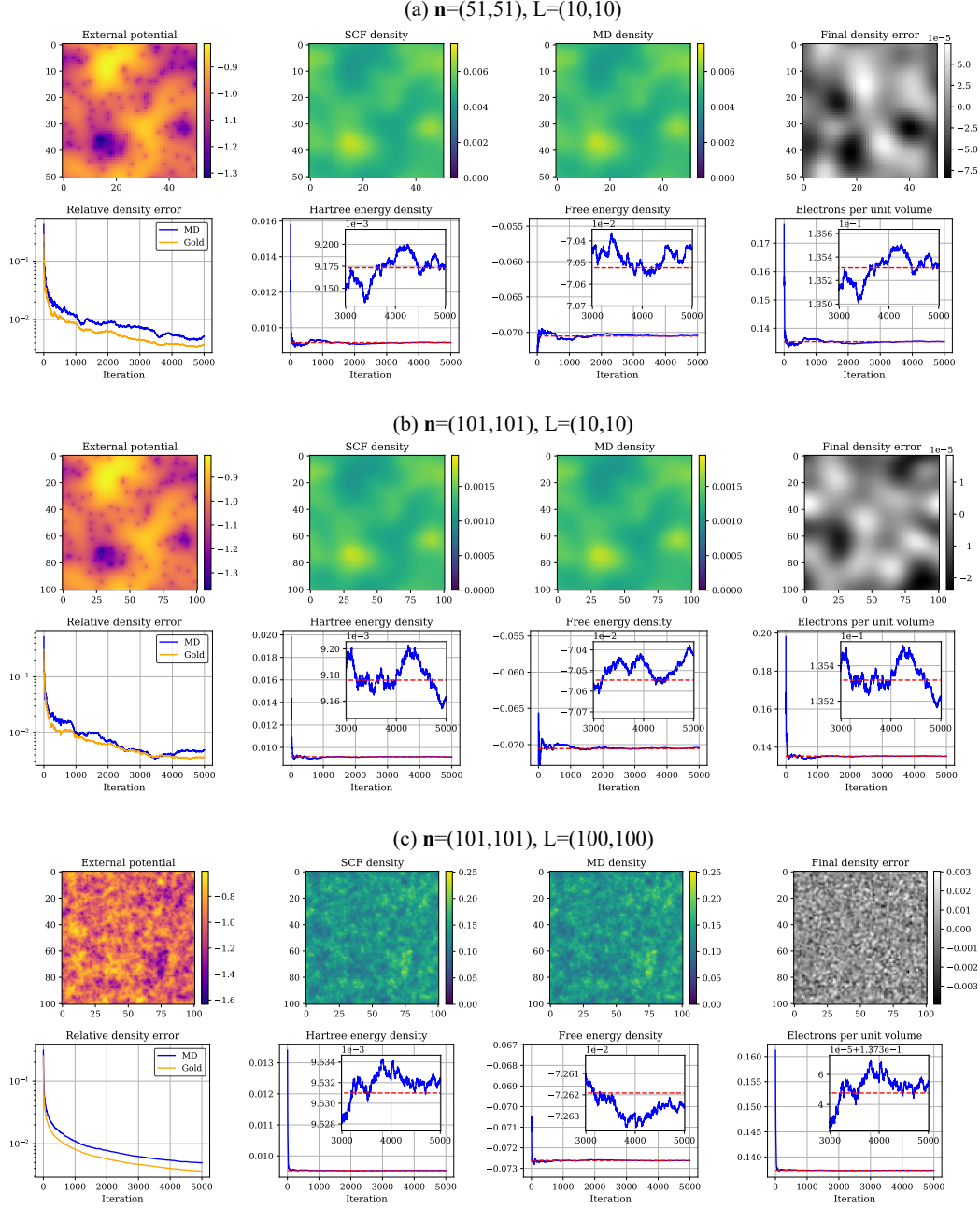


Figure 9.3: 2D simulation results of the mirror descent algorithm. We fix $\beta = 10$ and change the box size \mathbf{L} and grid size \mathbf{n} as indicated in the subplots. We use the red heatmap to show the external potential, the green heatmaps to show the density functions, and the gray heatmap to show the absolute error of density functions. The blue and gold lines denote the results of the mirror descent and the gold standard, while the red dashed lines denote the final outputs of the deterministic SCF.

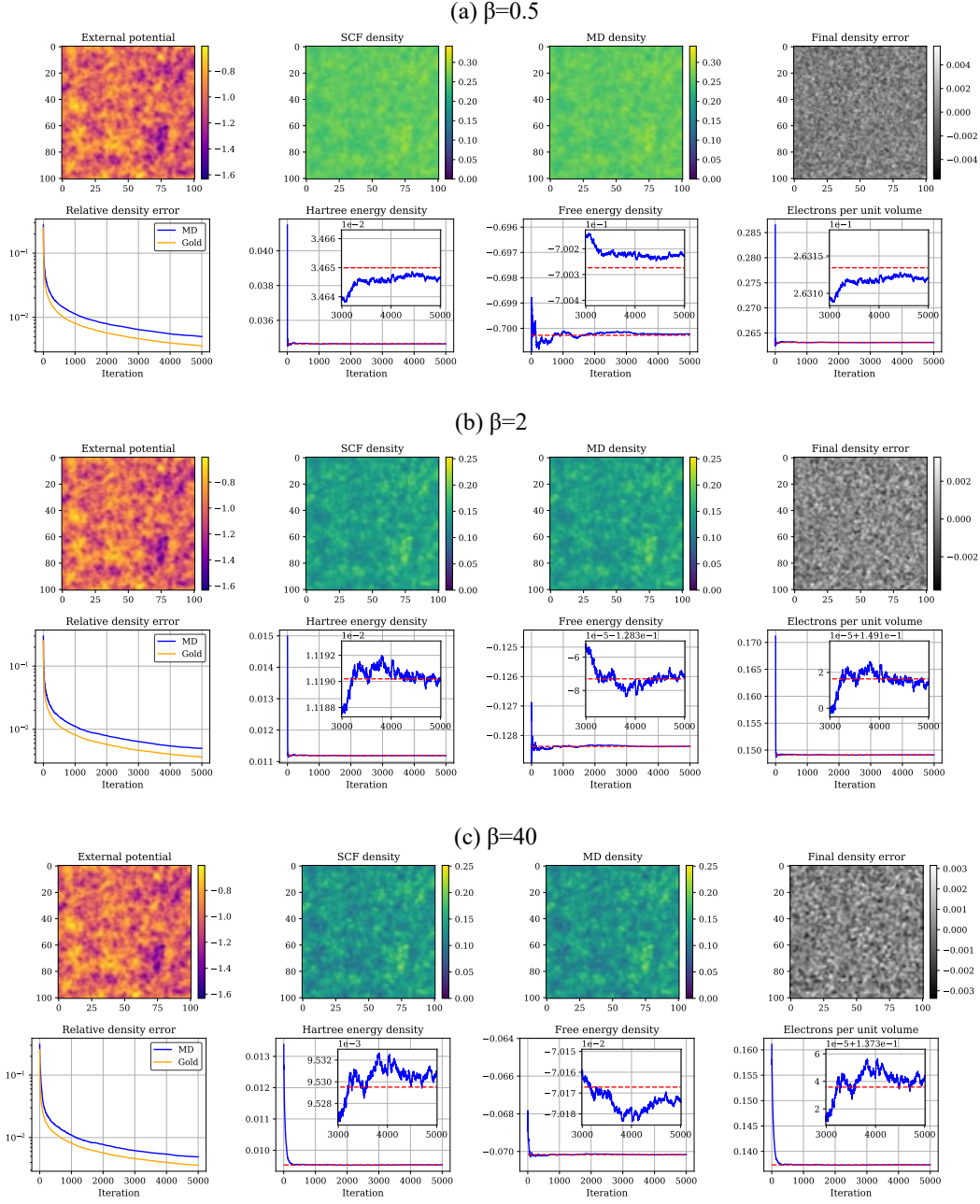


Figure 9.4: 2D simulation results of the mirror descent algorithm. We fix the grid size to be $\mathbf{n} = (101, 101)$ and the box size to be $\mathbf{L} = (100, 100)$. We consider $\beta = 0.5, 2, 40$. The other settings are the same as in Figure 9.3.

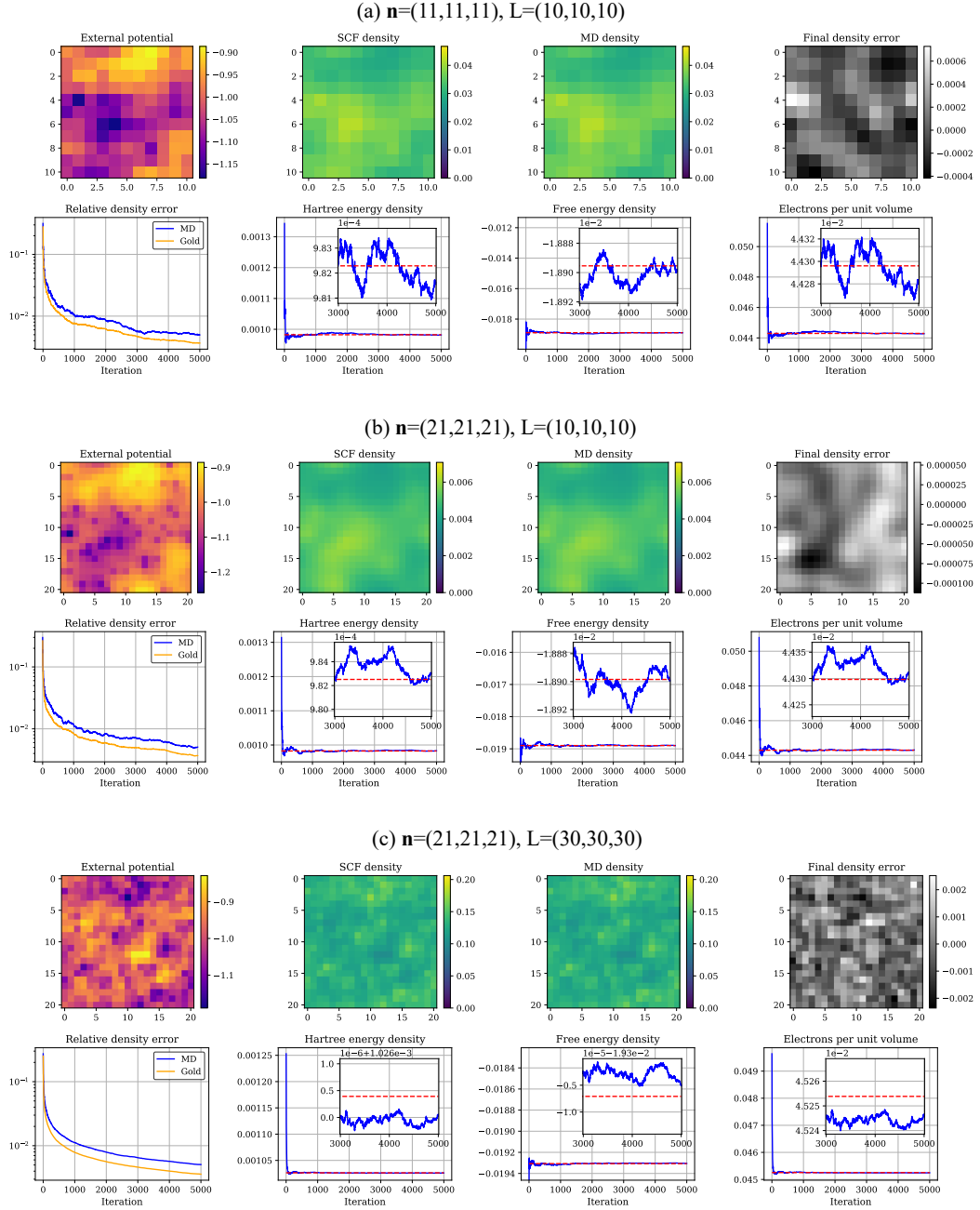


Figure 9.5: 3D simulation results of the mirror descent algorithm. Here we fix $\beta = 10$ and change the box size \mathbf{L} and grid size \mathbf{n} as indicated in the subplots. For the first row of each subplot, we show a slice of the external potential, density function, and the density errors. The other settings are the same as Figure 9.3.

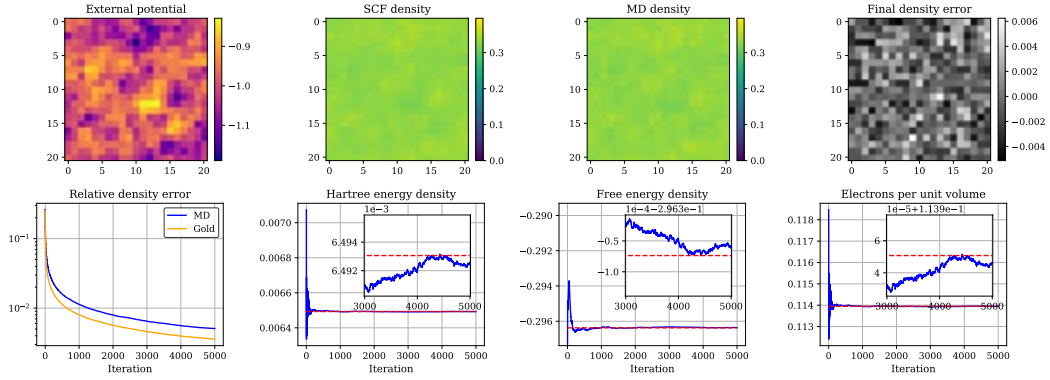
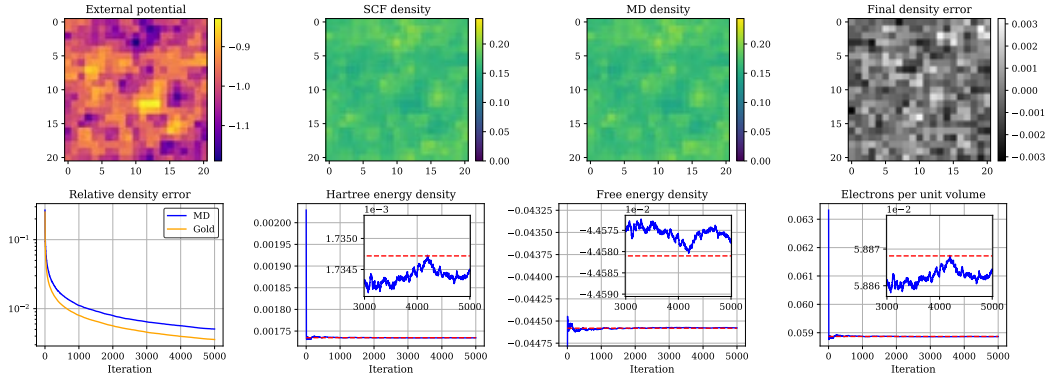
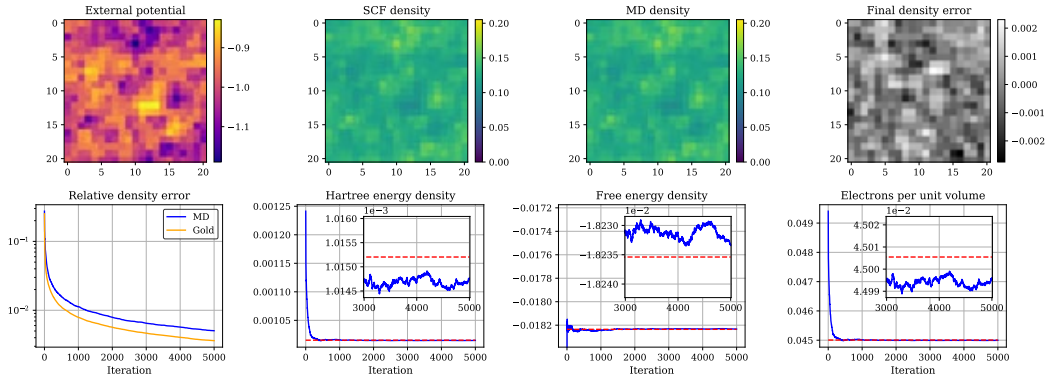
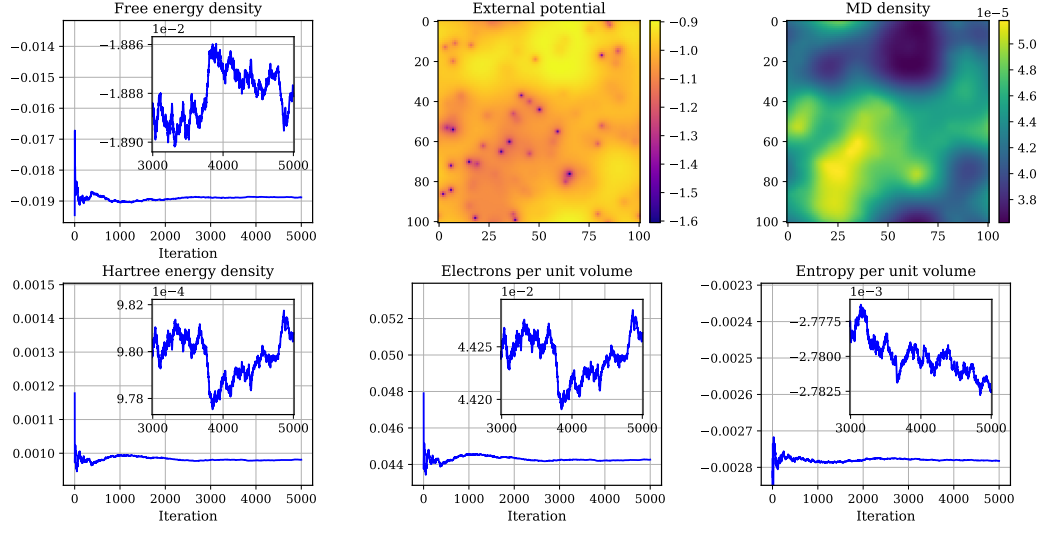
(a) $\beta=0.5$ (b) $\beta=2$ (c) $\beta=40$ 

Figure 9.6: 3D simulation results of the mirror descent algorithm. We fix the grid size to be $\mathbf{n} = (21, 21)$ and the box size to be $\mathbf{L} = (30, 30)$. We consider $\beta = 0.5, 2, 40$. The other settings are the same as in Figure 9.5.

(a) $\mathbf{n}=(101,101,101)$, $L=(10,10,10)$



(b) $\mathbf{n}=(101,101,101)$, $L=(100,100,100)$

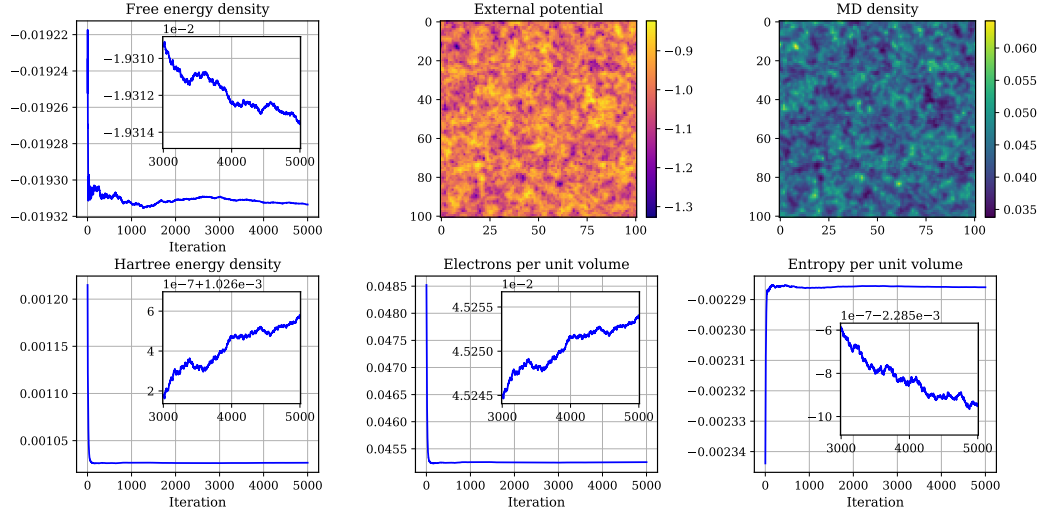


Figure 9.7: 3D simulation results of the mirror descent algorithm for two large systems. Here $\beta = 10$ and $\mathbf{n} = (101, 101, 101)$.

- [15] Edward G. Hohenstein, Robert M. Parrish, and Todd J. Martínez. Tensor hypercontraction density fitting. I. Quartic scaling second- and third-order Møller-Plesset perturbation theory. *The Journal of Chemical Physics*, 137(4):044103, 07 2012.
- [16] Edward G. Hohenstein, Robert M. Parrish, C. David Sherrill, and Todd J. Martínez. Communication: Tensor hypercontraction. III. Least-squares tensor hypercontraction for the determination of correlated wavefunctions. *The Journal of Chemical Physics*, 137(22):221101, 12 2012.
- [17] Michael F Hutchinson. A stochastic estimator of the trace of the influence matrix for laplacian smoothing splines. *Communications in Statistics-Simulation and Computation*, 18(3):1059–1076, 1989.
- [18] W. Kohn and L. J. Sham. Self-consistent equations including exchange and correlation effects. *Phys. Rev.*, 140:A1133–A1138, Nov 1965.
- [19] Guanghui Lan. An optimal method for stochastic composite optimization. *Mathematical Programming*, 133(1-2):365–397, June 2012.
- [20] Shaojie Li and Yong Liu. High probability guarantees for nonconvex stochastic gradient descent with heavy tails. In *International Conference on Machine Learning*, pages 12931–12963. PMLR, 2022.
- [21] L. Lin, M. Chen, C. Yang, and L. He. Accelerating atomic orbital-based electronic structure calculation via pole expansion and selected inversion. *J. Phys. Condens. Matter*, 25:295501, 2013.
- [22] L. Lin, J. Lu, L. Ying, R. Car, and W. E. Fast algorithm for extracting the diagonal of the inverse matrix with application to the electronic structure analysis of metallic systems. *Comm. Math. Sci.*, 7:755, 2009.
- [23] Lin Lin, Jianfeng Lu, Lexing Ying, and E Weinan. Pole-based approximation of the fermi-dirac function. *Chinese Annals of Mathematics, Series B*, 30(6):729–742, 2009.
- [24] Michael Lindsey. Fast randomized entropically regularized semidefinite programming, 2023.
- [25] Qianrui Liu and Mohan Chen. Plane-Wave-Based Stochastic-Deterministic Density Functional Theory for Extended Systems. *Physical Review B*, 106(12):125132, September 2022.
- [26] Zijian Liu, Ta Duy Nguyen, Thien Hang Nguyen, Alina Ene, and Huy Lê Nguyen. High Probability Convergence of Stochastic Gradient Methods, February 2023.
- [27] Haihao Lu, Robert M. Freund, and Yurii Nesterov. Relatively smooth convex optimization by first-order methods, and applications. *SIAM Journal on Optimization*, 28(1):333–354, 2018.
- [28] Jianfeng Lu and Lexing Ying. Compression of the electron repulsion integral tensor in tensor hypercontraction format with cubic scaling cost. *Journal of Computational Physics*, 302:329–335, 2015.
- [29] Raphael A Meyer, Cameron Musco, Christopher Musco, and David P Woodruff. Hutch++: Optimal stochastic trace estimation. *Proc SIAM Symp Simplicity Algorithms*, 2021:142–155, January 2021.

- [30] A. Nemirovski, A. Juditsky, G. Lan, and A. Shapiro. Robust Stochastic Approximation Approach to Stochastic Programming. *SIAM Journal on Optimization*, 19(4):1574–1609, January 2009.
- [31] Arkadi Nemirovski and David Yudin. Problem complexity and method efficiency in optimization, 1983.
- [32] Robert M. Parrish, Edward G. Hohenstein, Todd J. Martínez, and C. David Sherrill. Tensor hypercontraction. II. Least-squares renormalization. *The Journal of Chemical Physics*, 137(22):224106, 12 2012.
- [33] Attila Szabo and Neil S. Ostlund. *Modern Quantum Chemistry: Introduction to Advanced Electronic Structure Theory*. Dover Publications, Inc., Mineola, first edition, 1996.
- [34] Lloyd N Trefethen. *Approximation theory and approximation practice, extended edition*. SIAM, 2019.
- [35] Henk A Van der Vorst. Bi-cgstab: A fast and smoothly converging variant of bi-cg for the solution of nonsymmetric linear systems. *SIAM Journal on scientific and Statistical Computing*, 13(2):631–644, 1992.
- [36] Nuri Mert Vural, Lu Yu, Krishna Balasubramanian, Stanislav Volgushev, and Murat A. Erdogdu. Mirror Descent Strikes Again: Optimal Stochastic Convex Optimization under Infinite Noise Variance. In *Proceedings of Thirty Fifth Conference on Learning Theory*, pages 65–102. PMLR, June 2022.
- [37] Martin J Wainwright. *High-dimensional statistics: A non-asymptotic viewpoint*, volume 48. Cambridge University Press, 2019.
- [38] A. J. White and L. A. Collins. Fast and Universal Kohn-Sham Density Functional Theory Algorithm for Warm Dense Matter to Hot Dense Plasma. *Physical Review Letters*, 125(5):055002, July 2020.
- [39] Steven R. White. Hybrid grid/basis set discretizations of the schrödinger equation. *The Journal of Chemical Physics*, 147(24):244102, 12 2017.

Appendices

A Proofs for elementary facts (Section 3.4)

Proof of Lemma 2. We can verify by elementary computations that:

$$\begin{aligned} S_{\text{FD}}(X) &= n \left(\text{Tr} \left[\frac{X}{n} \log \left(\frac{X}{n} \right) \right] - \text{Tr} \left[\frac{X}{n} \right] \right) \\ &\quad + n \left(\text{Tr} \left[\frac{\mathbf{I}_n - X}{n} \log \left(\frac{\mathbf{I}_n - X}{n} \right) \right] - \text{Tr} \left[\frac{\mathbf{I}_n - X}{n} \right] \right) + n + n \log n \\ &= n S_{\text{VN}}(n^{-1}X) + n S_{\text{VN}}(n^{-1}[\mathbf{I}_n - X]) + n + n \log n, \end{aligned}$$

where $S_{\text{VN}}(Y) := \text{Tr}(Y \log Y) - \text{Tr}(Y)$ is the unnormalized von Neumann entropy on

$$\{Y : Y \succeq 0, \text{Tr}[Y] \leq 1\}.$$

Note that both X and $\mathbf{I}_n - X$ lie in this domain for $X \in \mathcal{X}$.

Now S_{VN} is 1-strongly convex with respect to $\|\cdot\|_*$ [5]. It is equivalent (cf., e.g., Proposition 1 of [27]) to say that the Hessian satisfies

$$\langle Z, \nabla^2 S_{\text{VN}}(Y) [Z] \rangle \geq \|Z\|_*^2.$$

But

$$\nabla^2 S_{\text{FD}}(X) = \frac{1}{n} \nabla^2 S_{\text{VN}}(n^{-1}X) + \frac{1}{n} \nabla^2 S_{\text{VN}}(n^{-1}[\mathbf{I}_n - X]),$$

and therefore

$$\langle Z, \nabla^2 S_{\text{FD}}(X) [Z] \rangle \geq \frac{2}{n} \|Z\|_*^2,$$

hence S_{FD} is $(2/n)$ -strongly convex with respect to $\|\cdot\|_*$. □

Proof of Lemma 3. First compute

$$S_{\text{FD}}(X_0) = \text{Tr} [\log(\mathbf{I}_n/2)] = -n \log 2.$$

Meanwhile it is straightforward to see that $S_{\text{FD}}(X) \leq 0$, since

$$x \log x + (1-x) \log(1-x) \leq 0$$

for all $x \in [0, 1]$. Finally, observe that $\nabla S_{\text{FD}}(X_0) = \log((\mathbf{I}_n/2)(\mathbf{I}_n/2)^{-1}) = 0$.

Then by definition

$$D(X \| X_0) = S_{\text{FD}}(X) - S_{\text{FD}}(X_0) - \langle \nabla S_{\text{FD}}(X_0), X - X_0 \rangle \leq n \log 2,$$

as was to be shown. □

B Proofs for sub-exponential concentration (Section 4.1)

Proof of Corollary 7. For $t \geq \frac{\nu}{2}$, we have that $e^{-\frac{t^2}{2\nu^2}} \leq e^{-\frac{t}{4\nu}}$. Therefore by Proposition 5, we have

$$\mathbb{P}[x \geq \mu + t \mid \mathcal{F}] \leq e^{-\frac{t}{4\nu}}$$

for all $t \geq \frac{\nu}{2}$. Since the right-hand side is deterministic, we can take the expectation of both sides and use the tower property of the conditional expectation to deduce that

$$\mathbb{P}[x \geq \mu + t] \leq e^{-\frac{t}{4\nu}}$$

for all $t \geq \frac{\nu}{2}$.

Therefore

$$\mathbb{P}\left[x \geq \mu + \frac{\nu}{2} + t\right] \leq e^{-\frac{(t+\nu/2)}{4\nu}} \leq e^{-\frac{t}{4\nu}}$$

for all $t \geq 0$.

Then solving $e^{-\frac{t}{4\nu}} = \delta$ for t , we see that

$$x \leq \mu + \frac{\nu}{2} + 4\nu \log(1/\delta)$$

with probability at least $1 - \delta$. □

Proof of Lemma 8. Throughout we will simply treat A as deterministic and aim to show that

$$\mathbb{E}\left[e^{\lambda(z^\top Az - \text{Tr}[A])}\right] \leq e^{\frac{(2\|A\|_F)^2 \lambda^2}{2}}, \quad \text{for all } |\lambda| \leq \frac{1}{4\|A\|}.$$

We can reduce to this case by disintegration.

Without loss of generality we can also let A be symmetric. (Otherwise, replace A with its symmetrization $\frac{1}{2}(A + A^\top)$, which leaves $z^\top Az$ unchanged and moreover cannot expand either the Frobenius or spectral norms.)

Use the spectral theorem to write $A = UEU^\top$ where U is orthogonal and $E = \text{diag}(\varepsilon_1, \dots, \varepsilon_n)$. Then

$$z^\top Az = (U^\top z)^\top E(U^\top z) = \sum_{i=1}^n \varepsilon_i \tilde{z}_i^2,$$

where $\tilde{z} := U^\top z$. Note that the components \tilde{z}_i are independent standard normal random variables.

It is well-known [37] that a squared standard normal random variable is sub-exponential with parameters $(2, 4)$, so

$$\begin{aligned} \mathbb{E}\left[e^{\lambda(z^\top Az - \text{Tr}[A])}\right] &= \mathbb{E}\left[e^{\lambda \sum_i \varepsilon_i (\tilde{z}_i^2 - 1)}\right] \\ &= \prod_{i=1}^n \mathbb{E}\left[e^{\lambda \varepsilon_i (\tilde{z}_i^2 - 1)}\right] \\ &\leq \prod_{i=1}^n e^{\frac{2^2 (\lambda \varepsilon_i)^2}{2}} \end{aligned}$$

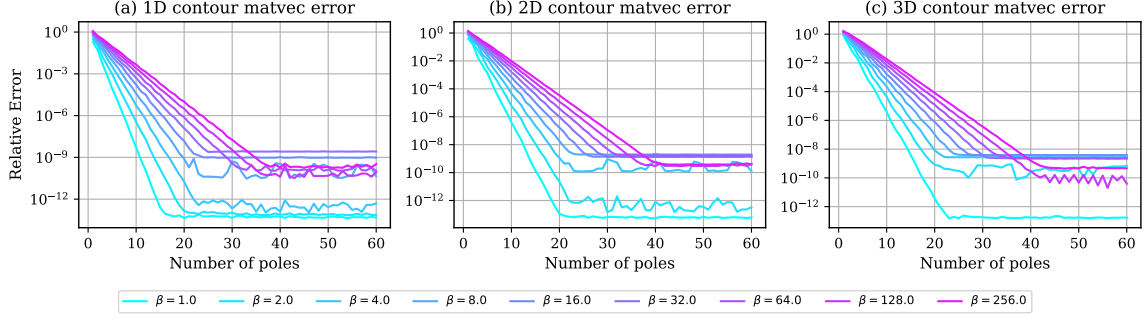


Figure C.1: Relative error of the contour matvec as a function of N_p for various spatial dimensions and inverse temperatures β . For the experiments, following the notation of Section 9, we set the grid sizes to $\mathbf{n} = 101$ for 1D, $(31, 31)$ for 2D, and $(11, 11, 11)$ for 3D, while the corresponding box sizes are $\mathbf{L} = 100$ for 1D, $\mathbf{L} = (30, 30)$ for 2D, and $\mathbf{L} = (10, 10, 10)$ for 3D. In generating the external potential, we use $\alpha = 0.5$ to define the Yukawa interaction. The matrix here is $C = K + U$, the vectors are random Gaussian samples, and the error is averaged over a sample size of $N_g = 10$.

as long as $|\lambda \varepsilon_i| \leq \frac{1}{4}$ for all i , which in particular holds as long as $|\lambda| \leq \frac{1}{4\|A\|}$, since $\|A\| = \max_i |\varepsilon_i|$. Then since in addition we have that $\|A_F\|^2 = \sum_{i=1}^n \varepsilon_i^2$, we continue our computation to deduce that

$$\mathbb{E} \left[e^{\lambda(z^\top A z - \text{Tr}[A])} \right] \leq e^{\frac{(2\|A\|_F)^2 \lambda^2}{2}},$$

meaning that $z^\top A z$ is sub-exponential with parameters $(2\|A\|_F, 4\|A\|)$. \square

C Contour integral details

We now discuss the use of contour integration to approximate matvecs by the square-root Fermi-Dirac function of the Hamiltonian, i.e., products of the form $X_t^{1/2} z = f_\beta^{1/2}(H_t) z$ for arbitrary vectors $z \in \mathbb{R}^n$. The idea, borrowed from [14], is to apply Cauchy's integral theorem to the holomorphic extension of $f_\beta^{1/2}$, i.e.,

$$f_\beta^{1/2}(H_t) z = \left[\int_{\partial\Gamma} g(s) (s\mathbf{I}_n - H_t)^{-1} ds \right] z \approx g_{N_p}(H_t) z := \sum_{i=1}^{N_p} w_i g(s_i) [(s_i\mathbf{I}_n - H_t)^{-1} z], \quad (\text{C.1})$$

where Γ is a good (smooth-boundaried) open region covering all the eigenvalues of H_t , g is a holomorphic extension of $f_\beta^{1/2}(x)$ from \mathbb{R} to Γ , N_p is the number of points used to discretize the contour integral, $s_i \in \partial\Gamma$ are the discretization points, and w_i are quadrature weights associated to s_i . Specifically, we apply the same contour and discretization as in PEXSI [23]. (See the rightmost panel of Figure C.2 below.)

Although it is not immediately obvious that such a holomorphic extension g exists, we will demonstrate that it does below in Appendix C.1.

Then the following theorem, whose proof is identical to its analogue from [23], bounds the error of this approach.

Theorem 32 (Section 2.2 of [23]). *There exists a constant C such that aforementioned contour integral approximation satisfies*

$$\|f_\beta^{1/2}(H_t) - g_{N_p}(H_t)\| = O(e^{-CN_p/\log(\beta\sigma(H))}),$$

where $\sigma(H)$ is the maximal singular value of H .

The plots in Figure C.1 validates this result, demonstrating consistent behavior across spatial dimensions and inverse temperatures.

C.1 Holomorphic extension

Now we focus on the construction of the holomorphic extension g adapted to the dumbbell contour depicted in the rightmost panel of Figure C.2. Note that it suffices to construct a holomorphic extension of $\log f_\beta$. Indeed, if $h(z)$ is a suitable holomorphic extension of $\log f_\beta$, then $\exp(h(z)/2)$ defines an extension for $f_\beta^{1/2}$.

Without loss of generality, we assume $\beta = 1$ via a horizontal scaling, since $f_\beta(x) = f_1(\beta x)$. Then for $\log f_1$, we construct h as:

$$h(z) := \begin{cases} \log f_1(z), & \text{if } \operatorname{Re}(z) \leq 0, \\ \log |1 + \exp(\beta z)| + i \cdot \left\{ \arg [1 + \exp(\beta z)] + 2\pi \left\lfloor \frac{\operatorname{Im}(z) - \pi}{2\pi} \right\rfloor \right\}, & \text{if } \operatorname{Re}(z) > 0. \end{cases}$$

Therefore, for $f_1^{1/2}$, we construct the holomorphic extension g as:

$$g(z) := \begin{cases} f_1^{1/2}(z), & \text{if } \operatorname{Re}(z) \leq 0, \\ |f_1^{1/2}(z)| \cdot \exp \left\{ i \left[\pi \left(1 - \left\lfloor \frac{\operatorname{Im}(z) - \pi/2}{\pi} \right\rfloor \right) + \frac{\arg [f_\beta(z)]}{2} \right] \right\}, & \text{if } \operatorname{Re}(z) > 0. \end{cases}$$

All these constructions are holomorphic on $\mathbb{C} \setminus \{iy \mid y \in (-\infty, -\pi] \cup [\pi, \infty)\}$, as illustrated in Figure C.2.

C.2 Solver and preconditioner

For our experiments outlined in Section 9, we use BiCGSTAB [35] to solve each linear system

$$(s_i \mathbf{I}_n - H_t)x = z$$

appearing in the right-hand side of (C.1).

In our periodic sinc basis, a nice property of the mirror descent update is that H_t can always be written as

$$H_t = c_t K + \operatorname{diag}^*(v_t),$$

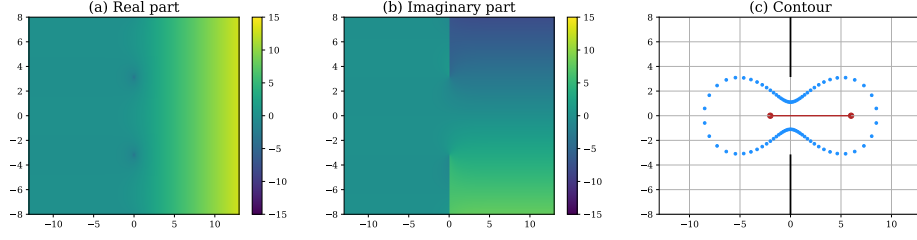


Figure C.2: Panels (a) and (b) together show the holomorphic extension of $-\log f_\beta(x)$. Panel (c) shows the 20 poles generated for the eigenvalue range $[-2, 6]$ and the inverse temperature $\beta = 1$.

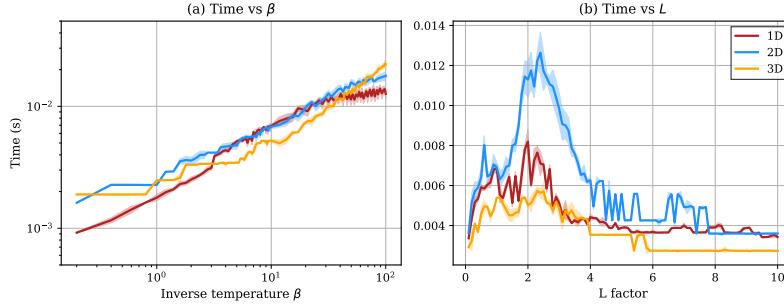


Figure C.3: Scaling of the wall clock time of a batch of $N_g = 20$ contour matvecs with respect to the inverse temperature and the box size. Here we choose the number of poles N_p to ensure that the relative error is about 10^{-5} . Following the notation of Section 9, the base choices of (\mathbf{n}, L) for 1D, 2D and 3D are $(101, 100)$, $((31, 31), 30)$, $((11, 11, 11), 10)$. In the right panel (b), the ‘ L factor’ indicates a scaling factor applied to the base box size L . (a) The log-log plot has a slope close to $1/2$, which indicates the scaling with respect to β is approximately $O(\sqrt{\beta})$. (b) Fixing $\beta = 10$, the results indicate that the time complexity is upper-bounded by a constant independent of the box size.

for some scalar $c_t \in \mathbb{R}$ and a suitable effective potential $v_t \in \mathbb{R}^n$. Let $\bar{v}_t \in \mathbb{R}$ denote the mean of the components of v_t . Then our choice of preconditioner in BiCGSTAB is defined by the linear map

$$x \mapsto (s_i \mathbf{I}_n - c_t K - \bar{v}_t \mathbf{I}_n)^{-1} x,$$

which permits log-linear implementation via FFT.

In Figure C.3, we report results indicating that the time complexity of the contour matvec scales as $O(\sqrt{\beta})$, independently of the box size.

C.3 Entropy term in the objective

We also use the contour integral technique to estimate the objective in order to plot the objective convergence of our algorithm.

To do so, we must explain how to estimate two additional terms: the single-electron term $\text{Tr}(CX_t)$ and the entropy term $\frac{1}{\beta}S_{\text{FD}}(X_t)$. The estimation of $\text{Tr}(CX_t)$ reuses the contour matvec results for the gradient estimation by rewriting:

$$\text{Tr}(CX_t) = \mathbb{E} \left\{ [f_\beta^{1/2}(H_t)z_t]^\top C [f_\beta^{1/2}(H_t)z_t] \right\}.$$

On the other hand, to estimate the entropy function, we must approximate an alternative matrix function. Indeed,

$$S_{\text{FD}}(X_t) = \mathbb{E} \left\{ z_t^\top [X_t \log X_t + (\mathbf{I}_n - X_t) \log(\mathbf{I}_n - X_t)] z_t \right\}.$$

Therefore, we aim to approximate the matvec

$$[X_t \log X_t + (I - X_t) \log(X_t)] z_t$$

For simplicity, we can focus on computing

$$[X_t \log X_t] z_t,$$

since the second term is analogous.

Since $X_t = f_\beta(H_t)$, we are motivated to apply the contour integration technique to a suitable holomorphic extension \tilde{g} of $f_\beta \log f_\beta$. But since we already constructed an extension for $\log f_\beta$, such an extension is recovered easily. Specifically, for $f_1 \log f_1$, we may construct \tilde{g} as:

$$\tilde{g}(z) := \begin{cases} f_1(z) \log f_1(z), & \text{if } \text{Re}(z) \leq 0, \\ -\frac{\log |1+\exp(z)| + i \cdot \left\{ \arg [1+\exp(z)] + 2\pi \left\lfloor \frac{\text{Im}(z) - \pi}{2\pi} \right\rfloor \right\}}{1+\exp(z)}, & \text{if } \text{Re}(z) > 0. \end{cases}$$

Indeed, this extension is also holomorphic on $\mathbb{C} \setminus \{iy \mid y \in (-\infty, -\pi] \cup [\pi, \infty)\}$. Hence, we can use the same contour and discretization as before. Then the linear solves can be recycled from the earlier computations and simply weighted differently to construct our objective estimator.

D Discussion of more general DFT

In general density functional theory, the energy consists of several components:

$$E(X) = \text{Tr}[CX] + E_{\text{hxc}}(X),$$

where

$$C_{ij} = \int \psi_i(x) \left[-\frac{1}{2}\Delta + v_{\text{ext}} \right] \psi_j(x) dx$$

denotes the matrix of the single-particle part of the quantum chemistry Hamiltonian in the $\{\psi_i\}$ basis, with v_{ext} denoting the diagonal external potential, and E_{hxc} denotes the Hartree and exchange-correlation contributions to the energy.

In turn,

$$E_{\text{hxc}}(X) = \tilde{E}(X) + E_{\text{xc}}(X)$$

consists of the Hartree energy which we have considered in this work as well as the *exchange-correlation* energy E_{xc} .

The exchange-correlation energy traditionally it only depends on X via the induced electron density ρ_X . (Notably, for example, hybrid functionals may more generally depend on X via the density matrix P_X .)

We comment that in particular, local density approximation (LDA) functionals have been used in stochastic DFT [12] and assume the form

$$E_{\text{xc}}(X) = \int \epsilon_{\text{LDA}}(\rho_X(x)) dx,$$

where ϵ_{LDA} could be a fairly arbitrary function $\mathbb{R} \rightarrow \mathbb{R}$. Under these circumstances, the exchange-correlation potential takes the form

$$\nabla E_{\text{xc}}(X) = \int \epsilon'_{\text{LDA}}(\rho_X(x)) \psi_i(x) \psi_j(x) dx.$$

In order to implement stochastic DFT with an LDA functional, one must construct ρ_X on a spatial grid and evaluate ϵ'_{LDA} pointwise to construct the LDA potential $\epsilon'_{\text{LDA}}(\rho_X(x))$ on the grid, which is then projected back to the basis. Note that this perspective is compatible with our definition of the vector $\rho(X)$, which can be interpreted (following the discussion of Section 6.2) as the vector of evaluations of the electron density on an interpolating grid.

There are two difficulties in extending our analysis to a more general setting. First of all, typically the exchange-correlation functional fails to be convex, and in fact many local optima may be present. (In particular, for LDA approximations, ϵ_{LDA} is not typically convex.) This seriously complicates the convergence theory for mirror descent, though it is reasonable to expect the theory to hold qualitatively locally near a local optimizer.

Second, as $\nabla E_{\text{xc}}(X)$ is not generally linear in X , the gradient estimator for the exchange-correlation potential will be biased, unlike our estimator for the Hartree potential $\nabla \tilde{E}(X)$. Therefore we do not enjoy the straightforward self-cancellation of estimation error over the optimization trajectory—captured in our analysis via the concentration inequality for martingale difference sequences (cf. Theorem 10).

However, we believe that the analysis of the Hartree case alone is crucial for understanding more general DFT. First of all, it is widely understood that the Hartree energy is the dominant contribution among the Hartree and exchange-correlation contributions. Although the exchange-correlation contribution is extremely relevant chemically, it is quantitatively much smaller, and therefore the estimation bias may be regarded as relatively small. If S shots are used in estimator for the density $\rho(X)$, then formally one expects the bias to scale as S^{-1} , with a preconstant proportional to the overall magnitude of exchange-correlation contribution. Meanwhile, the unbiased fluctuations (which scale as $S^{-1/2}$) will enjoy self-cancellation. Additionally, one might consider bias reduction techniques such as the jackknife [10] for reducing the bias to S^{-2} .

Moreover, it is possible to conceive of schemes for general stochastic DFT that solve the self-consistent Hartree theory as a subroutine, freezing the exchange-correlation potential within an inner loop in which the Hartree potential is optimized. Our convergence theory would be applicable to this inner loop. (We comment that similar two-loop strategies are used to converge the Hartree-Fock theory as well as DFT with hybrid functionals.) Since our convergence theory strikingly

suggests that converging the self-consistent Hartree theory to relative accuracy ε is about as easy as estimating the Hartree potential itself to relative accuracy ε , this separation of difficulties seems worthwhile. Meanwhile, the outer loop itself may be easier to converge quickly due to the relatively small magnitude of the exchange-correlation contribution. We leave the implementation and analysis of such directions to future work.

E Proofs for chemical potential optimization (Section 7)

Proof of Lemma 21. The supergradient is

$$\partial g_{N,\beta}(\mu) = N - \partial g_\beta(\mu),$$

where

$$\partial g_\beta(\mu) = \{\text{Tr}[X] : X \text{ is a minimizer of } F_\beta(X) - \mu \text{Tr}[X]\}.$$

Hence for $\beta < +\infty$, the function $g_{N,\beta}$ is differentiable, but in any case $g_{N,\beta}$ is Lipschitz with Lipschitz constant n , since $N - \text{Tr}[X] \in [-n, n]$ for any X satisfying $0 \preceq X \preceq \mathbf{I}_n$. \square

Proof of Lemma 22. Let us define

$$a := \lambda_{\min}(C) - c_h - \beta^{-1} \log(\gamma^{-1})$$

and

$$b := \lambda_{\max}(C) + c_h + \beta^{-1} \log([1 - \gamma]^{-1})$$

as the left and right endpoints of our desired bounding interval.

Suppose first that $\beta < +\infty$. We know that any optimizer μ must satisfy $N = \text{Tr}[X_{\beta,\mu}]$ where $X_{\beta,\mu}$ is the optimizer of (2.1). But recall (3.3), i.e., that

$$X_{\beta,\mu} = f_\beta(\nabla E(X_{\beta,\mu}) - \mu \mathbf{I}_n).$$

We use the fact that

$$f_\beta(x) = \frac{1}{1 + e^{\beta x}} \leq e^{-\beta x}$$

for all x to deduce that

$$\text{Tr}[X_{\beta,\mu}] \leq \text{Tr}[\exp(-\beta[\nabla E(X_{\beta,\mu}) - \mu \mathbf{I}_n])].$$

Now $\nabla E(X) = C + \nabla \tilde{E}(X) \succeq C - c_h \mathbf{I}_n$ by Lemma 1, so it follows that

$$\text{Tr}[X_{\beta,\mu}] \leq e^{\beta(\mu - \lambda_{\min}(C) + c_h)} n,$$

meaning that $\mu \geq a$. This gives the desired lower bound for μ .

Similarly, using the inequality

$$f_\beta(x) = 1 - f_\beta(-x) \geq 1 - e^{\beta x},$$

we deduce that

$$\text{Tr}[X_{\beta,\mu}] \geq n - \text{Tr}[\exp(\beta[\nabla E(X_{\beta,\mu}) - \mu \mathbf{I}_n])],$$

which in turn implies that

$$1 - \gamma \leq e^{\beta(\lambda_{\max}(C) + c_h - \mu)},$$

i.e., that $\mu \leq b$. This gives the desired upper bound for μ .

These arguments show that any maximizer must be attained in the desired interval. But let us verify concretely that a maximizer is in fact attained. Indeed, note that the same arguments show that if $\mu > a$ holds strictly, then for any $X_{\beta,\mu}$ solving (2.1), we have $\text{Tr}[X_{\beta,\mu}] > N$, i.e., $g'_{N,\beta}(\mu) < 0$. Likewise if $\mu < b$ holds strictly, then for any $X_{\beta,\mu}$ solving (2.1), we have $\text{Tr}[X_{\beta,\mu}] < N$, i.e., $g'_{N,\beta}(\mu) > 0$. Together these facts guarantee that in fact the maximum must be attained on the interval appearing in the statement of the theorem.

Now consider the limiting case $\beta = +\infty$. The same arguments show that if $\mu \leq a$, then $\nabla E(X) - \mu \mathbf{I}_n \succeq 0$ for all $X \in \mathcal{X}$ (and likewise that if $\mu < a$, then $\nabla E(X) - \mu \mathbf{I}_n \succ 0$). Therefore if $\mu \leq a$, then $X = 0$ is an optimizer of (2.1) (unique if $\mu < a$). Similarly, if $\mu \geq b$, then $X = \mathbf{I}_n$ is an optimizer of (2.1) (unique if $\mu > b$).

It follows from (7.1) and (7.2) that if $\mu \leq a$, then $g_{N,\beta}(\mu) = N\mu$, and if $\mu \geq b$, then $g_{N,\beta}(\mu) = (N - n)\mu$. Thus $g_{N,\beta}$ is non-decreasing for $\mu \leq a$ and non-increasing for $\mu \geq b$. It follows that a maximum is attained in $[a, b]$. \square

Proof of Proposition 23. By Theorem 17, we know that

$$\max_{k=0,\dots,M} \left| \frac{\hat{g}_{N,\beta,k}}{n} - \frac{g_{N,\beta}(\mu_k)}{n} \right| \leq O \left(\frac{c_h \log(KTm/\delta)}{\sqrt{T}} + \frac{\|C\| + c_h + \beta^{-1} \log([\gamma(1-\gamma)]^{-1})}{T} \right) \quad (\text{E.1})$$

holds with probability at least $1 - \delta$, where we have used the fact that

$$\mu_k \in [\lambda_{\min}(C) - c_h - \beta^{-1} \log[\gamma^{-1}], \lambda_{\max}(C) + c_h + \beta^{-1} \log([1 - \gamma]^{-1})],$$

so

$$\|C - \mu_k \mathbf{I}_n\| = O \left(\frac{\|C\| + c_h + \beta^{-1} \log([\gamma(1-\gamma)]^{-1})}{T} \right)$$

for all k .

Recall from Lemma 21 that $g_{N,\beta}(\mu_k)$ is Lipschitz with constant n . Moreover, the spacing $h = \mu_{k+1} - \mu_k$ satisfies

$$h \leq \frac{2\|C\| + 2c_h + \beta^{-1} \log([\gamma(1-\gamma)]^{-1})}{M}.$$

Let μ_\star denote an optimizer of $g_{N,\beta}$. We know by Lemma 22 that there must exist some k such that $|\mu_k - \mu_\star| \leq h/2$. Thus the result follows from Lipschitzness and (E.1). \square

F Proofs for complete basis set limit (Section 8)

Proof of Lemma 25. Similarly to the proof of Lemma 2, we can verify by elementary computations that:

$$\begin{aligned} S_{\text{FD}}(X) &= \tau \left(\text{Tr} \left[\frac{X}{\tau} \log \left(\frac{X}{\tau} \right) \right] - \text{Tr} \left[\frac{X}{\tau} \right] \right) \\ &\quad + \tau \left(\text{Tr} \left[\frac{\mathbf{I}_n - X}{\tau} \log \left(\frac{\mathbf{I}_n - X}{\tau} \right) \right] - \text{Tr} \left[\frac{\mathbf{I}_n - X}{\tau} \right] \right) + n + n \log \tau \\ &= \tau S_{\text{VN}}(\tau^{-1} X) + \tau S_{\text{VN}}(\tau^{-1} [\mathbf{I}_n - X]) + n + n \log \tau, \end{aligned}$$

where $S_{\text{VN}}(Y) := \text{Tr}(Y \log Y) - \text{Tr}(Y)$ is the unnormalized von Neumann entropy on

$$\{Y : Y \succeq 0, \text{Tr}[Y] \leq 1\}.$$

Assuming that $X \in \mathcal{X}_\tau$, we have that $\text{Tr}[X/\tau] \leq 1$, i.e., $\tau^{-1}X$ must lie in this domain for the von Neumann entropy.

Now S_{VN} is 1-strongly convex with respect to $\|\cdot\|_*$ [5]. It is equivalent (cf., e.g., Proposition 1 of [27]) to say that the Hessian satisfies

$$\langle Z, \nabla^2 S_{\text{VN}}(Y) [Z] \rangle \geq \|Z\|_*^2.$$

But

$$\nabla^2 S_{\text{FD}}(X) = \frac{1}{\tau} \nabla^2 S_{\text{VN}}(\tau^{-1} X) + \frac{1}{\tau} \underbrace{\nabla^2 S_{\text{VN}}(\tau^{-1} [\mathbf{I}_n - X])}_{\succeq 0}.$$

We do not have a nonzero lower bound for the second term, but we do not need it. (The zero lower bound simply follows from convexity.)

It follows that

$$\langle Z, \nabla^2 S_{\text{FD}}(X) [Z] \rangle \geq \frac{1}{\tau} \|Z\|_*^2,$$

hence S_{FD} is $(1/\tau)$ -strongly convex with respect to $\|\cdot\|_*$. □

Proof of Lemma 26. Following the proof of Lemma 11, we have that $[\hat{\rho}_t]_q$ is sub-exponential with parameters $(2[\rho(X_t)]_q, 4[\rho(X_t)]_q)$. Hence by applying Corollary 7 with $\nu = 2c_\Psi$, we deduce that

$$[\hat{\rho}_t]_q \leq [\rho(X_t)]_q (2 + 8 \log(Tm/\delta))$$

holds with probability at least $1 - \frac{\delta}{Tm}$.

Then (applying absolute value bars entrywise) it follows that

$$|V \hat{\rho}_t| \leq |V| \hat{\rho}_t \leq |V| \rho(X_t) (2 + 8 \log(Tm/\delta)),$$

hence by the definition of \tilde{c}_h we have (8.3)

$$\|V \hat{\rho}_t\|_\infty \leq \tilde{c}_h (2 + 8 \log(Tm/\delta)).$$

Then it follows that

$$\|\hat{G}_t\| = \|\Psi^\top \text{diag}^*[V\hat{\rho}_t]\Psi\| \leq \|V\hat{\rho}_t\|_\infty \leq 2(1 + 4\log(Tm/\delta))\tilde{c}_h$$

holds for all $t = 0, \dots, T-1$ with probability at least $1 - \delta$, as was to be shown. \square

Proof of Lemma 27. . Let $Y = X_\star - X_t$, and let $y = \langle \Delta_t, Y \rangle$. As in the proof of Lemma 12, we have that y is sub-exponential with parameters $(2\|A\|_F, 4\|A\|)$, conditioned on \mathcal{F}_{t-1} , where $A := X_t^{1/2}\nabla\tilde{E}(Y)X_t^{1/2}$.

We can split $A = A_1 - A_2$, where $A_1 = X_t^{1/2}\nabla\tilde{E}(X_\star)X_t^{1/2}$ and $A_2 = X_t^{1/2}\nabla\tilde{E}(X_t)X_t^{1/2}$. Now

$$\|A_1\| = \|X_t^{1/2}\nabla\tilde{E}(X_\star)X_t^{1/2}\| \leq \|X_t^{1/2}\|^2 \|\nabla\tilde{E}(X_\star)\| \leq \|\nabla\tilde{E}(X_\star)\|,$$

where we have used the fact that $\|X_t\| \leq 1$ in the last inequality.

Now

$$\begin{aligned} \|\nabla\tilde{E}(X_\star)\| &= \|\Psi^\top \text{diag}^*[V\rho(X_\star)]\Psi\| \\ &\leq \|V\rho(X_\star)\|_\infty \\ &\leq \tilde{c}_h, \end{aligned}$$

so $\|A_1\| \leq \tilde{c}_h$, and similar reasoning shows $\|A_2\| \leq \tilde{c}_h$, hence

$$\|A\| \leq 2\tilde{c}_h.$$

Moreover,

$$\begin{aligned} \|A_1\|_F^2 &= \text{Tr} \left[\nabla\tilde{E}(X_\star)X_t\nabla\tilde{E}(X_\star)X_t \right] \\ &= \left\langle \left(\nabla\tilde{E}(X_\star)X_t \right)^\top, \nabla\tilde{E}(X_\star)X_t \right\rangle \\ &\leq \|\nabla\tilde{E}(X_\star)X_t\|_F^2 \\ &\leq \|\nabla\tilde{E}(X_\star)\|^2 \|X_t\|_F^2 \\ &\leq \tilde{c}_h^2 \|X_t\|_F^2, \end{aligned}$$

so $\|A_1\|_F \leq \tilde{c}_h \|X_t\|_F$ and similar reasoning shows $\|A_2\|_F \leq \tilde{c}_h \|X_t\|_F$. Therefore

$$\|A\|_F \leq 2\tilde{c}_h \|X_t\|_F,$$

which completes the proof. \square

Proof of Lemma 29. Recall that

$$X_0 = f_\beta(H_0),$$

where $H_0 = C - \mu \mathbf{I}_n$, so

$$\begin{aligned} \text{Tr}[X_0] &= \sum_{k=1}^n f_\beta(\lambda_k(H_0)) \\ &= \sum_{k < c_\lambda \mu} f_\beta(\lambda_k(H_0)) + \sum_{k \geq c_\lambda \mu} f_\beta(\lambda_k(H_0)) \\ &\leq c_\lambda \mu + \sum_{k \geq c_\lambda \mu} e^{-\beta \lambda_k(H_0)} \\ &\leq c_\lambda \mu + e^{\beta \mu} \sum_{k \geq c_\lambda \mu} e^{-\beta \lambda_k(C)}, \end{aligned}$$

where we have used the fact that $f_\beta(x) \leq \max(1, e^{-\beta x})$ for all x .

Then Assumption 2 implies in turn that

$$\begin{aligned} \text{Tr}[X_0] &\leq c_\lambda \mu + e^{\beta \mu} \sum_{k \geq c_\lambda \mu} e^{-(\beta/c_\lambda)k} \\ &= c_\lambda \mu + \frac{1}{1 - e^{-(\beta/c_\lambda)}}, \end{aligned}$$

where we have used the geometric sum formula and the fact that the first term in the geometric series is bounded above by $e^{-\beta \mu}$.

Then we can use the general inequality $\frac{1}{1 - e^{-1/x}} \leq (1 + x)$, which holds for $x \geq 0$, to deduce that

$$\text{Tr}[X_0] \leq c_\lambda \mu + (1 + \beta^{-1} c_\lambda) = c_\lambda (\mu + \beta^{-1}) + 1.$$

□

Proof of Lemma 29. First expand

$$D(X_\star \| X_0) = S_{\text{FD}}(X_\star) - S_{\text{FD}}(X_0) + \beta \langle C - \mu \mathbf{I}_n, X_\star - X_0 \rangle.$$

Now $S_{\text{FD}} \leq 0$ always, so immediately we have

$$D(X_\star \| X_0) \leq -S_{\text{FD}}(X_0) + \beta \langle C, X_\star - X_0 \rangle. \quad (\text{F.1})$$

Let us first bound the first term. Since $X_0 = f_\beta(C - \mu \mathbf{I}_n)$, we can expand

$$-S_{\text{FD}}(X_0) = \sum_{k=1}^n g(\lambda_k(C) - \mu),$$

where

$$g(x) := -f_\beta(x) \log f_\beta(x) - [1 - f_\beta(x)] \log[1 - f_\beta(x)].$$

Now g admits the elementary pointwise bound

$$g(x) \leq e^{-\beta|x|/3}$$

for all $x \in \mathbb{R}$, so

$$\begin{aligned} -S_{\text{FD}}(X_0) &\leq \sum_{k=1}^n e^{-\frac{\beta}{3}|\lambda_k(C)-\mu|} \\ &= \sum_{k < c_\lambda \mu} e^{-\frac{\beta}{3}|\lambda_k(C)-\mu|} + \sum_{k \geq c_\lambda \mu} e^{-\frac{\beta}{3}|\lambda_k(C)-\mu|} \\ &\leq c_\lambda \mu + e^{\beta\mu/3} \sum_{k \geq c_\lambda \mu} e^{-\frac{\beta}{3c_\lambda}k} \end{aligned}$$

where we have used Assumption 2 in the last line. Then by summing the geometric series and copying the argument at the end of the proof of Lemma 29, we obtain the bound

$$\begin{aligned} -S_{\text{FD}}(X_0) &\leq c_\lambda \mu + \frac{1}{1 - e^{-\frac{\beta}{3c_\lambda}}} \\ &\leq c_\lambda \mu + (1 + 3\beta^{-1}c_\lambda) \\ &= c_\lambda(\mu + 3\beta^{-1}) + 1. \end{aligned} \tag{F.2}$$

Now we turn to bounding the term $\langle C - \mu \mathbf{I}_n, X_\star - X_0 \rangle$ appearing on the right-hand side of (F.1). It is useful to recall (3.3), i.e., that the optimizer X_\star satisfies

$$X_\star = f_\beta(C - \mu \mathbf{I}_n + V_\star), \quad \text{where } V_\star := \nabla \tilde{E}(X_\star).$$

Then write

$$\begin{aligned} \langle C, X_\star - X_0 \rangle &= \langle C, X_\star \rangle - \langle C, X_0 \rangle \\ &= \langle C - \mu \mathbf{I}_n, X_\star \rangle - \langle C - \mu \mathbf{I}_n, X_0 \rangle + \mu \text{Tr}[X_\star - X_0]. \\ &\leq \langle C - \mu \mathbf{I}_n, X_\star \rangle - \langle C - \mu \mathbf{I}_n, X_0 \rangle, \end{aligned}$$

where in the last line we use the fact that $\text{Tr}[X_\star] \leq \text{Tr}[X_0]$, which follows from the same argument demonstrating that $\text{Tr}[X_t] \leq \text{Tr}[X_0]$ in the proof of Theorem 28.

Then we can further manipulate:

$$\begin{aligned} \langle C, X_\star - X_0 \rangle &\leq \langle C - \mu \mathbf{I}_n + V_\star, X_\star \rangle - \langle C - \mu \mathbf{I}_n, X_0 \rangle - \langle V_\star, X_\star \rangle \\ &\leq \langle C - \mu \mathbf{I}_n + V_\star, X_\star \rangle - \langle C - \mu \mathbf{I}_n, X_0 \rangle, \end{aligned}$$

where in the last line we have used the fact that $V_\star \succeq 0$ (following from Assumption 1).

Then we conclude that

$$\langle C, X_\star - X_0 \rangle \leq \text{Tr}[h(H_\star) - h(H_0)],$$

where $H_0 = C - \mu \mathbf{I}_n$, $H_\star = C - \mu \mathbf{I}_n + V_\star$, and we define

$$h(x) := x f_\beta(x).$$

Then expand in terms of eigenvalues to obtain

$$\begin{aligned}
\langle C, X_\star - X_0 \rangle &\leq \sum_{k=1}^n [h(\lambda_k(C + V_\star) - \mu) - h(\lambda_k(C) - \mu)] \\
&= \sum_{k < c_\lambda \mu} [h(\lambda_k(C + V_\star) - \mu) - h(\lambda_k(C) - \mu)] \\
&\quad + \sum_{k \geq c_\lambda \mu} [h(\lambda_k(C + V_\star) - \mu) - h(\lambda_k(C) - \mu)]. \tag{F.3}
\end{aligned}$$

Now it can be verified that h is 2-Lipschitz (independent of β), so the first sum on the right-hand side of (F.3) is bounded as

$$\begin{aligned}
&\sum_{k < c_\lambda \mu} [h(\lambda_k(C + V_\star) - \mu) - h(\lambda_k(C) - \mu)] \\
&\leq 2 \sum_{k < c_\lambda \mu} |\lambda_k(C + V_\star) - \lambda_k(C)| \\
&\leq 2c_h c_\lambda \mu, \tag{F.4}
\end{aligned}$$

where we have used Weyl's theorem and the fact that $\|V_\star\| \leq c_h$.

Finally, we concentrate on the second sum on the right-hand side of (F.3). Note that for $k \geq c_\lambda \mu$, Assumption (2) implies that $\lambda_k(C) - \mu \geq 0$, hence $h(\lambda_k(C) - \mu) \geq 0$, hence we can simplify by dropping the second summand:

$$\begin{aligned}
&\sum_{k \geq c_\lambda \mu} [h(\lambda_k(C + V_\star) - \mu) - h(\lambda_k(C) - \mu)] \\
&\leq \sum_{k \geq c_\lambda \mu} h(\lambda_k(C + V_\star) - \mu).
\end{aligned}$$

Next observe the elementary inequality $\frac{x}{1+e^x} \leq e^{-x/2}$, which holds for all $x \in \mathbb{R}$. It follows that

$$h(x) = \frac{x}{1+e^{\beta x}} \leq \beta^{-1} e^{-\beta x/2}$$

for all x . Thus

$$\begin{aligned}
\sum_{k \geq c_\lambda \mu} h(\lambda_k(C + V_\star) - \mu) &\leq \beta^{-1} \sum_{k \geq c_\lambda \mu} e^{-\beta[\lambda_k(C + V_\star) - \mu]} \\
&\leq \beta^{-1} \sum_{k \geq c_\lambda \mu} e^{-\beta[\lambda_k(C) - \mu]} \\
&\leq \beta^{-1} e^{\beta \mu} \sum_{k \geq c_\lambda \mu} e^{-(\beta/c_\lambda)k}
\end{aligned}$$

where in the penultimate line we have used the fact that $\lambda_k(C + V_\star) \geq \lambda_k(C)$, which follows from Weyl's monotonicity theorem. Then by the same geometric series argument as the one at the end of the proof of Lemma 29, it follows that the second sum on the right-hand side of (F.3) is bounded by

$$\beta^{-1} (1 + \beta^{-1} c_\lambda).$$

Combining this fact with the bound (F.4) for the first sum on the right-hand side of (F.3) and substituting into (F.3), we conclude that

$$\langle C, X_\star - X_0 \rangle \leq 2c_{\text{h}}c_\lambda\mu + \beta^{-1}(1 + \beta^{-1}c_\lambda).$$

Therefore, combining with (F.1) and (F.2), we obtain

$$D(X_\star || X_0) \leq c_\lambda(\mu + 2\beta c_{\text{h}}\mu + 4\beta^{-1}) + 2.$$

□